The Plant Cell, Vol. 21: 1212–1229, April 2009, www.plantcell.org

A Mobile Secretory Vesicle Cluster Involved in Mass Transport from the Golgi to the Plant Cell Exterior [W][OA]

Kiminori Toyooka,[a] Yumi Goto,[a] Satoru Asatsuma,[a,b] Masato Koizumi,[a] Toshiaki Mitsui,[c] and Ken Matsuoka[a,b,1]

[a] RIKEN Plant Science Center, Tsurumi-ku, Yokohama 230-0045, Japan
[b] Laboratory of Plant Nutrition, Faculty of Agriculture, Kyushu University, Higashi-ku, Fukuoka 812-8581, Japan
[c] Laboratories of Plant and Microbial Genome Control, Graduate School of Science and Technology, Niigata University, Ikarashi, Nishi-ku, Niigata 950-2181, Japan

Secretory proteins and extracellular glycans are transported to the extracellular space during cell growth. These materials are carried in secretory vesicles generated at the trans-Golgi network (TGN). Analysis of the mammalian post-Golgi secretory pathway demonstrated the movement of separated secretory vesicles in the cell. Using secretory carrier membrane protein 2 (SCAMP2) as a marker for secretory vesicles and tobacco (*Nicotiana tabacum*) BY-2 cell as a model cell, we characterized the transport machinery in plant cells. A combination of analyses, including electron microscopy of quick-frozen cells and four-dimensional analysis of cells expressing fluorescent-tagged SCAMP2, enabled the identification of a clustered structure of secretory vesicles generated from TGN that moves in the cell and eventually fuses with plasma membrane. This structure was termed the secretory vesicle cluster (SVC). The SVC was also found in *Arabidopsis thaliana* and rice (*Oryza sativa*) cells and moved to the cell plate in dividing tobacco cells. Thus, the SVC is a motile structure involved in mass transport from the Golgi to the plasma membrane and cell plate in plant cells.

INTRODUCTION

The division and expansion of cells requires trafficking of lipids, proteins, and polysaccharides to the plasma membrane (PM) and extracellular space. These molecules are synthesized and/or modified in the Golgi apparatus and sorted into secretory vesicles at the trans-Golgi network (TGN) for transport to the PM.

The Golgi apparatus in plants differs from that in mammals in several aspects, including spatial organization, dynamic properties, and functional activity. Numerous Golgi apparatus are dispersed throughout the cytoplasm in plant cells and move along actin cytoskeletal elements (Nebenfuhr et al., 1999). One function of the plant Golgi apparatus is as the factory for noncellulose extracellular glycans, including hemicellulose and pectin (Cosgrove, 2005). Rapidly dividing plant cells need to synthesize large quantities of these glycans and contain several hundred to thousands of Golgi stacks (Nebenfuhr et al., 1999).

The unique features of the plant Golgi apparatus also reflect a difference in the secretory machinery between plants and mammals. Mammalian and yeast cells share a similar transport system for secretory vesicles (Bednarek and Falbel, 2002), and the sorting of proteins at the late secretory pathway is influenced by early, late, and recycling endosomes. In plant cells, the prevacuolar compartments (PVCs), multivesicular bodies (MVBs), partially coated reticulum, tubuvesicular endosomes, and vacuoles are involved in secretion and are collectively termed the post-Golgi compartments (Surpin and Raikhel, 2004; Lam et al., 2007b). However, it is not yet clear whether these are the sole elements in the late secretory pathway of plants and how they interact during the secretory process.

Electron microscopy observations of high-pressure frozen cells have indicated that isolated TGN-like structures or post-Golgi vesicle clusters are found in a number of plant cells (Samuels et al., 2002; Saint-Jore-Dupas et al., 2004, Staehelin and Kang, 2008). In recent years, various trafficking components in plant cells have also been genetically characterized (Rojo and Denecke, 2008); however, functional analysis of these structures and trafficking components has been limited by the lack of suitable molecular markers in this compartment.

Secretory vesicles contain divergent classes of molecules: not only the soluble protein cargo, but also membrane proteins that are involved in the trafficking process itself. One group of proteins that has been identified as a component of secretory vesicles are the secretory carrier membrane proteins (SCAMPs) (Brand et al., 1991; Takamori et al., 2006). The conserved structure of SCAMPs consists of a cytoplasmic N-terminal domain with repeated asparagin-proline-phenylalanine (NPF) sequences, four transmembrane regions, and a cytoplasmic tail (Fernandez-Chacon and Sudhof., 2000). Genome-wide analysis has shown that plants also possess a SCAMP gene family (Fernandez-Chacon and Sudhof, 2000), and analysis of rice (*Oryza sativa*) SCAMP1 revealed an involvement endocytosis (Lam et al., 2007a, 2007b).

In this article, we investigated the tobacco (*Nicotiana tabacum*) SCAMP2 protein based on its putative function in the late secretory pathway. Fluorescent tagging and immunoelectron

[1] Address correspondence to kenmat@agr.kyushu-u.ac.jp.
The author responsible for distribution of materials integral to the findings presented in this article in accordance with the policy described in the Instructions for Authors (www.plantcell.org) is: Ken Matsuoka (kenmat@agr.kyushu-u.ac.jp).
[W]Online version contains Web-only data.
[OA]Open Access articles can be viewed online without a subscription.
www.plantcell.org/cgi/doi/10.1105/tpc.108.058933

microscopy (immuno-EM) analyses of tobacco BY-2 cells revealed that SCAMP2 is localized in the PM, the TGN, and a mobile structure that we term the secretory vesicle cluster (SVC). Analysis of the SVC using total internal reflection fluorescence microscopy, four-dimensional confocal laser scanning microscopy, and SCAMP2 as a marker demonstrated that it matures from a tubulovesicular structure that might be identical to or is derived from the TGN. Moreover, the SVC was observed to fuse with the PM in nondividing cells and to be targeted to the cell plate in dividing cells. Based on these results, we propose that the SVC is a mobile compartment containing SCAMP2 that is involved in mass transport from the Golgi apparatus to the cell exterior in plants.

RESULTS

Subcellular Localization of Tobacco SCAMP2

To obtain a deeper understanding of endomembrane organelles in plant cells, we have been characterizing membrane proteins potentially involved in vesicular trafficking as suggested by transcriptomic analysis of tobacco BY-2 cells (Matsuoka et al., 2004). Polyclonal antibodies developed against candidate proteins were used to compare their distribution in BY-2 cells with that of organelle markers (Figure 1; Matsuoka et al., 1997). One of these proteins, a tobacco SCAMP homolog (referred to as SCAMP2; see below), displayed a unique distribution pattern on sucrose gradients for subcellular fractionation (Figure 1). Because its fractionation pattern corresponded to localization to the PM and Golgi apparatus, SCAMP2 was chosen for further analysis.

The anti-SCAMP2 antibody recognized two closely associated bands of ~29 kD and a band of 27 kD that were present in identical membrane fractions of tobacco BY-2 cells at varied intensity ratios. Similar multiple bands were observed with antibodies against mammalian SCAMP2 (Liu et al., 2002) and SCAMP2-yellow fluorescent protein (YFP) in BY-2 cells (described below), suggesting that the signals observed in Figure 1 were specific for the tobacco SCAMP homolog(s) and an accurate representation of its distribution. Little signal was found in the higher molecular weight regions in the same immunoblot, suggesting that the antibody raised against tobacco SCAMP2 is specific for the protein. The sequence of the encoding full-length cDNA and deduced SCAMP2 protein was then determined. Based on amino acid sequence comparison with other species, the tobacco SCAMP homolog was classified as a member of the SCAMP2 family and thus is hereafter referred to as SCAMP2 (see Supplemental Figure 1 online). Interestingly, the C-terminal Tyr motif was only found in the plant homologs (see Supplemental Figure 1 online).

Staining of tobacco BY-2 cells with anti-SCAMP2 antibody followed by confocal laser scanning microscopy (CLSM) analysis

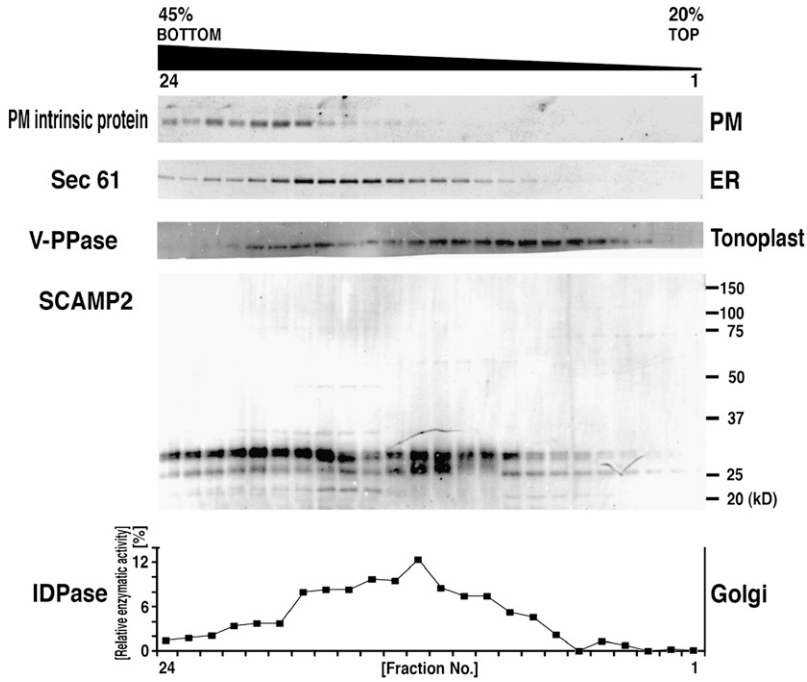

Figure 1. Distribution of SCAMP2 within Endomembrane Organelles.

Microsomes were prepared from BY-2 cells in the presence of Mg^{2+} and subjected to isopycnic sucrose density gradient ultracentrifugation. The resulting gradients were fractionated from the bottom into 24 fractions. The concentration of sucrose in the gradient is shown at the top. The distribution of marker proteins was analyzed by immunoblotting with specific antibodies, against PM intrinsic protein for PM, Sec61 for the ER, and V-PPase for the vacuolar membrane. The enzyme activity of inosine disphosphatase (IDPase) as a marker for the Golgi apparatus was measured. The distribution of SCAMP2 was analyzed by immunoblotting with anti-SCAMP2 antibody.

revealed strong fluorescence at intracellular dot structures (Figure 2A). The PM and cell plates were also stained with this antibody, although the signals at the PM were sometimes obscure. Localization in the PM and at intracellular dots was also observed for fusion proteins of SCAMP2 with monomeric red fluorescent protein (mRFP) and with YFP in tobacco BY-2 cells (Figure 2B). Colocalization of signals in the same intracellular dots and PM was also observed when both fusion constructs were coexpressed in the same BY-2 cell (Figure 2B) and when BY-2 cells expressing SCAMP2-YFP were stained with anti-SCAMP2 antibody (Figure 2C). In addition, analysis of SCAMP2-YFP subcellular localization by cell fractionation showed a similar distribution in the gradient and a similar multiple band pattern as the endogenous SCAMP2, corresponding to the PM and Golgi fractions (Figure 2D). These results confirmed that the SCAMP2-YFP fusion protein correctly represents localization of endogenous SCAMP2.

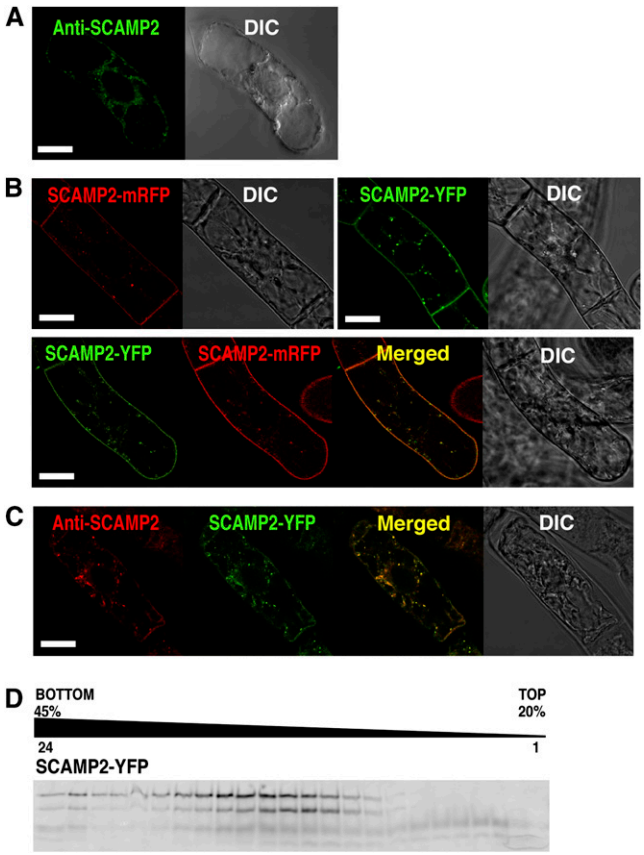

Figure 2. Subcellular Localization of SCAMP2 by CLSM.

(A) Immunolocalization of SCAMP2 in BY-2 cells using an anti-SCAMP2 antibody.

(B) Localization of SCAMP2-mRFP and SCAMP2-YFP fusion proteins in BY-2 cells.

(C) Immunofluorescence labeling of BY-2 cells expressing SCAMP2-YFP using anti-SCAMP2 antibody. Bars = 10 μm in **(A)** to **(C)**.

(D) The distribution of SCAMP2-YFP analyzed by subcellular fractionation. Proteins in microsomal membranes prepared from SCAMP2-YFP expressing BY-2 cells and separated by isopycnic sucrose density gradient ultracentrifugation were separated by SDS-PAGE and fluorescence of SCAMP2-YFP in the polyacrylamide gel was detected using a fluoroimager.

To test if the SCAMP2-containing dot structure could be an endosomal organelle, the localization of SCAMP2-YFP was compared with that of the endosomal marker dye FM4-64 by confocal microscopy (Figure 3A). Cells were stained with 33 μM FM4-64 on ice and washed with cold medium, after which they were returned to room temperature to resume intracellular trafficking. At early stages (5 to 10 min) after FM4-64 incubation, we observed dotted structures of FM4-64 signals in a background weak fluorescence signal showing similar pattern to cytosol stained by 5- (and 6-) chloromethyl SNARF-1 (Yuasa et al., 2005). The cytosolic pattern was clearly distinct from the pattern of the endoplasmic reticulum (ER) (see Supplemental Figure 2A online). Lower concentration of FM4-64 (17 μM) showed an essentially identical pattern (see Supplemental Figure 2B online). The dotted structures emitting strong red FM4-64 fluorescence rarely colocalized with YFP signals in major population of the cells (9% ± 5.9% colocalization, $n = 7$ cells; Figure 3A, top), whereas a minor population of cells showed more frequent colocalization (63% ± 11% colocalization, $n = 4$ cells). After 30 to 40 min, there was a uniform and high colocalization between the YFP-positive SCAMP2-YFP dots and FM4-64 positive dots (88% ± 6.2%, $n = 10$; Figure 3A, middle). At later stages (90 to 120 min), FM4-64 was transported to vacuolar membranes, whereas SCAMP2-YFP was not detected at the tonoplast (Figure 3A, bottom). Cells stained at room temperature with FM4-64 and AM4-65 (a fixable analog of FM4-64; Lam et al., 2008) showed strong staining of the PM, followed by appearance of FM4-64 (Figure 3B) and AM4-65 (Figure 3C) positive dots at 5 to 10 min after incubation that mainly colocalized with SCAMP2-YFP. These results suggest that the styrl dye–stained PM was rapidly internalized into the plant cells at room temperature and colocalized with SCAMP2-positive dots.

Following internalization, FM4-64 fluorescence is transported to the Golgi apparatus in addition to endosomes and vacuolar membranes (Bolte et al., 2004; Dettmer et al., 2006). The possibility that the SCAMP2-positive dots represented the Golgi apparatus was therefore investigated. We have previously reported that prolyl hydroxylase (PH) cycles between the ER and the Golgi apparatus and is predominantly found in the *cis*-located cisternae of the Golgi (Yuasa et al., 2005). This feature was used to mark the *cis*-Golgi by coexpressing a PH-mRFP fusion protein together with SCAMP2-YFP (Figure 4A). Many, but not all, of the YFP-positive dots were localized in close proximity to the mRFP signals (Figure 4B) and were seen moving together in the cell when traced using a confocal time-lapse scanning program (Figure 4C). Based on these results, we predicted that a significant proportion of SCAMP2 would localize to the TGN or to organelles located near the *trans*-cisternae of the Golgi apparatus. When internalization of FM4-64 was observed in BY-2 cells expressing a fusion protein of PH with green fluorescent protein (GFP), FM4-64 signals were detected on the sides of the Golgi apparatus after 30 to 40 min of incubation (see Supplemental Figure 3A online). These observations strongly suggest that the SCAMP2-positive dots showing the FM4-64 signal in Figure 3 represent the trans-Golgi cisternae or the TGN.

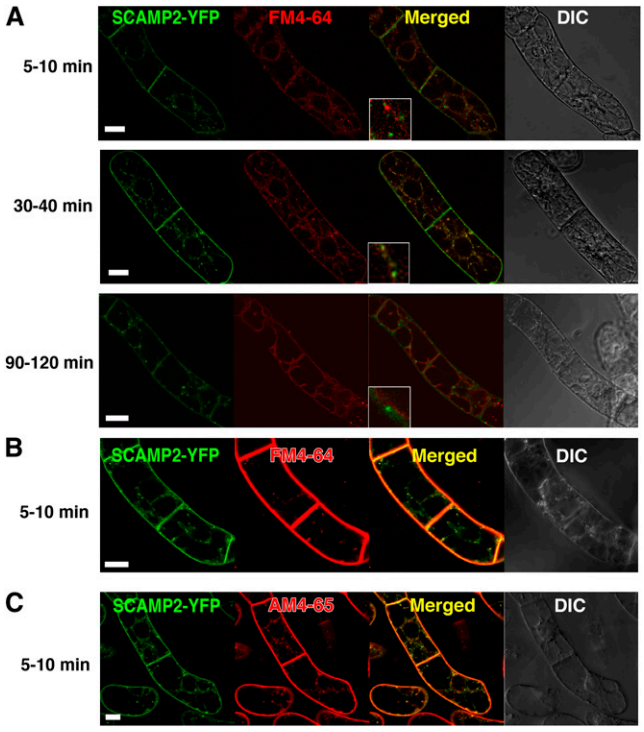

Figure 3. Subcellular Localization of SCAMP2 with Styryl Fluorescent Dyes.

Distribution of endocytotic marker dyes FM4-64 and AM4-65 in BY-2 cells expressing SCAMP2-YFP.

(A) Cells were incubated with medium containing FM4-64 on ice for 10 min and then washed with cold medium. Samples were then incubated at room temperature for 5 to 10 min, 30 to 40 min, and 90 to 120 min before collecting fluorescent images.

(B) Cells were incubated with medium containing FM4-64 for 2 min at room temperature, washed with medium, and then incubated at room temperature. Samples were observed 5 to 10 min after washing.

(C) Distribution of AM4-65 in BY-2 cells expressing SCAMP2-YFP. The cells were incubated with medium containing AM4-65 for 2 min at room temperature, washed with medium, and then incubated at room temperature. The samples were observed 5 to 10 min after washing. Bars = 20 μm.

We next investigated whether SCAMP2 also localizes to the post-Golgi component in the plant secretory pathway. In *Arabidopsis thaliana*, the SNARE proteins SYP22 and SYP41 localize to the membranes of the MVB/PVC/vacuoles and trans-Golgi/TGN, respectively (Uemura et al., 2004; Foresti et al., 2006). Fusion proteins containing YFP together with tobacco SYP22 or tobacco SYP41 were expressed in BY-2 cells and showed fluorescence patterns conceptually identical to that seen in *Arabidopsis* (see Supplemental Figures 3B and 3C online). Coexpression of the SNARE protein fusions with SCAMP2-mRFP revealed a colocalization between YFP-SYP41 and SCAMP2-mRFP positive dots (Figure 4D). Most, but not all, of the SCAMP2-mRFP positive dots showed YFP-SYP41 positive signal (91% ± 3% colocalization, $n = 5$ cells), although some of the YFP-SYP41 positive structures did not contain SCAMP2-mRFP, as the percentage of green dots showing red fluorescence was a little lower in the same cells (80% ± 18% colocalization, $n = 5$ cells). This observation suggests that most of the SCAMP2 and SYP41 localized in the same compartment, but some population of each of them localized in compartments where the other is absent.

In contrast with SYP41, YFP-SYP22 fluorescence did not colocalize with SCAMP2-mRFP signals (Figure 4E), although YFP-SYP22 fluorescence frequently colocalized with FM4-64 signals (see Supplemental Figure 3C online). These results indicated that SCAMP2 does not accumulate in the MVB/PVC post-Golgi compartment.

It has been reported that the Ypt3/Rab11 subfamily of Rab GTPases is localized in TGN and subsequent secretory compartments (Chow et al., 2008). We isolated the tobacco *Rab11D* cDNA and expressed the protein as a fusion with mRFP in the BY-2 cells. mRFP-Rab11D fluorescence almost completely colocalized with GFP-Pra3, which is reported to localize in TGN (Inaba et al., 2002) (see Supplemental Figure 3D online). Coexpression of mRFP-Rab11D and SCAMP2-YFP indicated that the fluorescence dots of both proteins colocalized in the same compartment about half the time (47% ± 5.9% colocalization, $n = 4$ cells), but some dots were independent (Figure 4F). These results are consistent with localization of SCAMP2 in the TGN and organelles involved in the secretory pathway.

To confirm the involvement of SCAMP2 in the secretory pathway, SCAMP2-YFP and PH-mRFP localization was studied in the presence of Brefeldin A (BFA). BFA inhibits transport vesicle formation at the Golgi apparatus and other membranes in the secretory pathway. After 2 h in the presence of a low concentration of BFA (5 μg/mL), SCAMP2-YFP had moved to the PM and PH-mRFP was redistributed from the Golgi to the ER (Figure 5A). We also analyzed the effect of wortmannin, which at 10 to 100 μM inhibits the biosynthesis of both phosphatidylinositol 3- and 4- phosphates as well as phospholipids in tobacco BY-2 cells (Matsuoka et al., 1995a). It was reported recently that wortmannin at 16.5 μM induces a morphological change of rice SCAMP1 positive compartments in tobacco BY-2 cells from a punctate structure to a ring shape (Lam et al., 2007a). By contrast, even in the presence of the same concentration of wortmannin, most SCAMP2-YFP structures remained punctate, with <1% assuming a ring shape structure in transformed BY-2 cells (see Supplemental Figure 4 online). These data confirmed that SCAMP2-positive dots are not the *cis*-Golgi, PVC/MVB, and rice SCAMP1 positive endosomal organelles. Furthermore, these observations suggest that the tobacco SCAMP2 and rice SCAMP1 trafficking pathways in tobacco BY-2 cells are not identical.

We next investigated whether SCAMP2 recycles between the trans-Golgi/TGN and the PM. Cells expressing both SCAMP2-YFP and PH-mRFP were first treated with 5 μg/mL BFA for 2 h to remove the signal from intracellular dot-shaped compartments (Figure 5A). Cells were then washed with fresh medium without BFA and transferred to medium containing cycloheximide (CHX), a potent inhibitor of protein synthesis. After 1 h, cells contained intracellular dots emitting both YFP and mRFP fluorescence (Figure 5B), and the percentage of YFP signal showing internal localization increased from 3.7 to 32.9% (Figure 5D). The relative percentage of internal YFP signal after washing out BFA in both

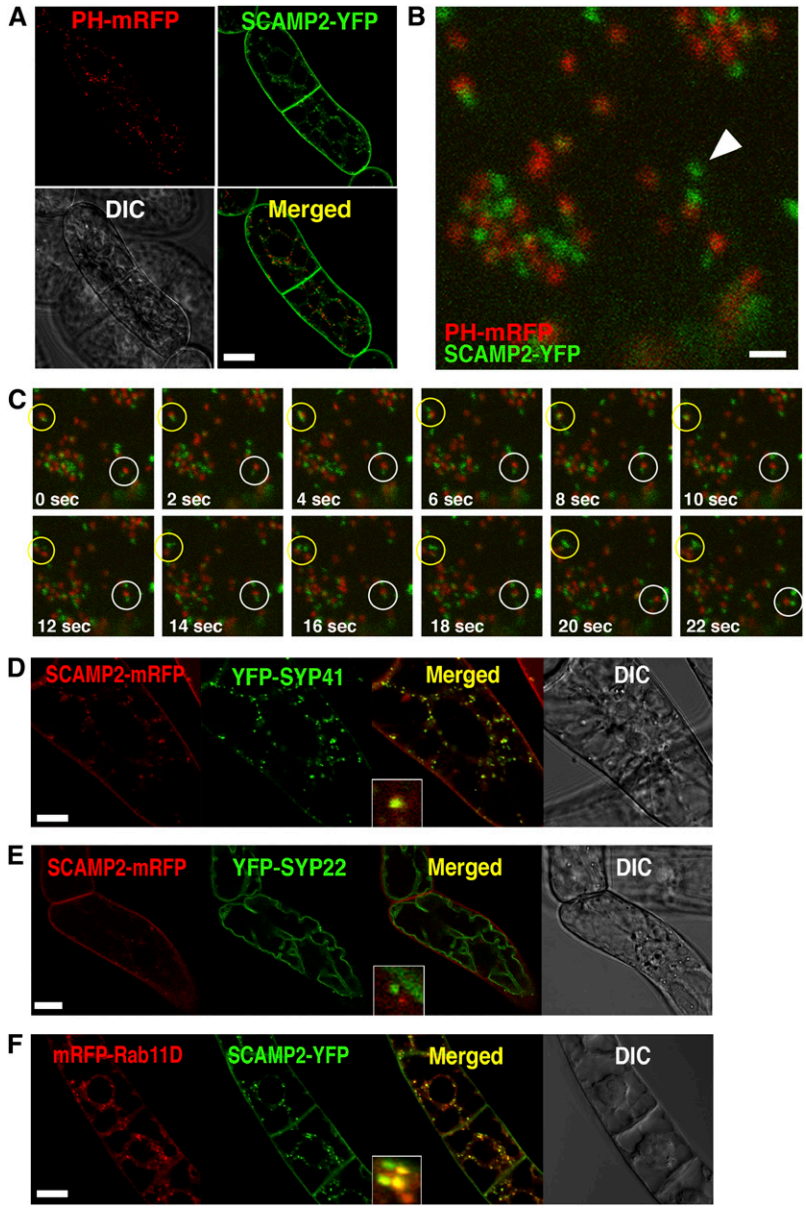

Figure 4. Subcellular Localization of SCAMP2 with Organelle Markers.

(A) to **(C)** *cis*-Golgi was marked with PH-mRFP, and SCAMP2-YFP was expressed in the same cells.
(A) Lower magnification.
(B) Higher magnification. The arrowhead shows a YFP dot independent from PH-mRFP. Bar = 2 μm.
(C) Time-lapse pictures of **(B)**. Most of the YFP and mRFP dots are moving side by side (white circle). Several YFP dots are touching and running together (yellow circle).
(D) to **(F)** Localization of YFP-SYP41 with SCAMP2-mRFP **(D)**, YFP-SYP22 with SCAMP2-mRFP **(E)**, and SCAMP2-YFP with mRFP-Rab11D **(F)**. Bars = 20 μm in **(A)** and **(D)** to **(F)**.

the presence and absence of CHX did not differ significantly to that of cells without any treatment (Figure 5D). This observation indicates that SCAMP2 had moved to the trans-Golgi/TGN or another intracellular compartment from the PM after removal of BFA. This redistribution was investigated further using 2,3-butanedione monoxime, which is a general myosin ATPase inhibitor (Higaki et al., 2006) that can inhibit endocytosis mediated by the actin-myosin system (Samaj et al., 2004). Treatment with 2,3-butanedione monoxime for an hour after washing of BFA-treated cells prevented the increase in internal YFP fluorescence and resulted in SCAMP2-YFP signal remaining almost exclusively at the PM (Figures 5C and 5D), whereas some of the

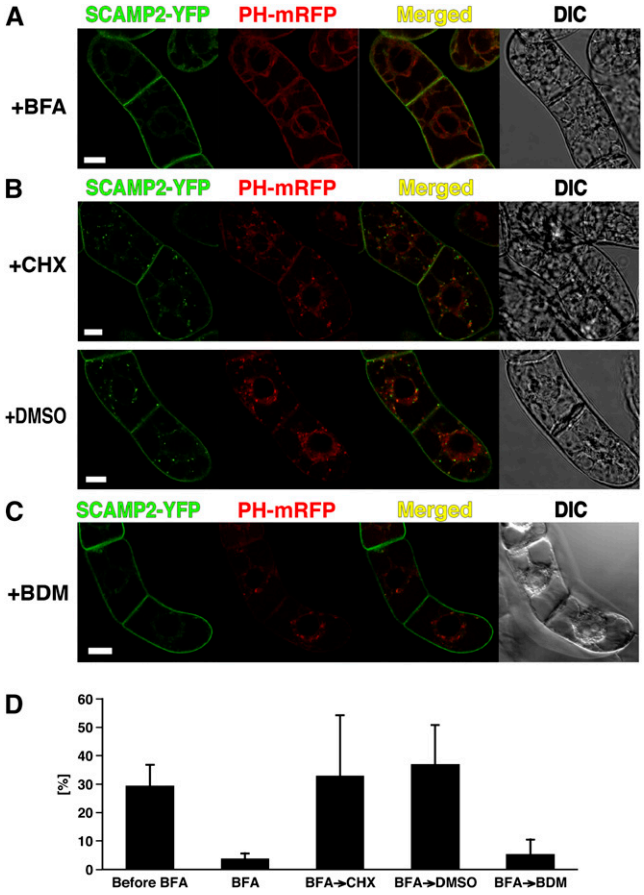

Figure 5. Subcellular Localization of SCAMP2 in the Presence of Inhibitors.

(A) Effects of BFA. BY-2 cells expressing PH-mRFP and SCAMP2-YFP were treated with 5 μg/mL of BFA for 120 to 140 min.

(B) Recovery from BFA treatment. After BY-2 cells expressing SCAMP2-YFP and PH-mRFP had been treated with 5 μg/mL of BFA for 2 h, they were washed and transferred to fresh growth medium containing 50 μM CHX or DMSO alone as a negative control for 1 h.

(C) Recovery from BFA treatment in the presence of a myosin inhibitor, 2,3-butanedione monoxime (BDM). BY-2 cells expressing SCAMP2-YFP were treated with BFA for 2 h and then washed and transferred to fresh medium containing 20 mM 2,3-butanedione monoxime and incubated for 1 h. Bars = 20 μm in **(A)** to **(C)**.

(D) Quantification of SCAMP2-YFP signals before and after various treatments. Percentage of intracellular YFP signals was shown. Error bars indicate SD.

PH-mRFP positive dots reappeared in the cell. These results suggested that SCAMP2 likely returns to the trans-Golgi/TGN or intracellular dot structures from the PM in a myosin-dependent manner.

Characterization of SCAMP2-Containing Compartments

The nature of the SCAMP2-containing structures was studied in further detail using immuno-EM. Ultrathin sections of BY-2 cells were prepared by high-pressure freezing/freeze substitution (HPF/FS) and stained using an anti-SCAMP2 antibody and immunogold labeling. Gold particles were present at the PM, the TGN, and in clusters of vesicles (Figures 6A to 6C; see Supplemental Figures 5A to 5D online). The clusters generally contained 5 to 12 vesicles of ~50 to 100 nm in diameter. Consistent with the fluorescence colocalization experiments, gold particles were not detected in the MVBs and small vacuoles (Figure 6A). These results indicated that the SCAMP2 positive fluorescence dots correspond to the TGN and to a vesicle cluster not associated with the Golgi apparatus. These vesicle clusters were termed the SVCs, as vesicles in this structure contained secretory markers, such as secretory GFP and pectin (described below), and the morphology of this structure was distinct from TGN (described below). The ultrastructure of the Golgi apparatus, TGN, and SVC were next compared by staining with tannic acid, which enhances the contrast of membrane structures rich in glycoprotein as well as coat proteins of transport vesicles. The observed tannic acid-enhanced ultrastructure of the TGN and SVC was consistent with the observation that SVC and TGN were stained with an antibody that recognized complex glycans (Figures 6D to 6H). Some clusters of vesicles existed on one side of the Golgi stacks where the TGN was localized (Figure 6F; see Supplemental Figure 6A online), and vesicles in the TGN sometimes had structures of clathrin-coated vesicles (CCVs) and clathrin-coated buds (Figure 6G). By contrast, few clathrin coats were detected on SVCs, especially those located close to PM (Figures 6H and 6I). Thin-section images of both showed that SVCs and TGNs contained similar numbers of vesicles (6.9 and 7.8, respectively; Figure 6I, left). By contrast, the average numbers of CCVs in each SVC was significantly lower than that in each TGN (0.31 and 1.4, respectively; Figure 6I, right). The TGN tended to have thick tubules in addition to vesicles with luminal space (Figure 6G), whereas SVCs, particularly those located close to the PM, did not display thick tubules and only occasionally contained a thin tubule in addition to the vesicles (Figure 6B and H). These observations indicated that the TGN and SVCs are related, but are distinct compartments in the cell.

To confirm that SVCs exist as structures separate from the Golgi stacks and the TGN, BY-2 cells expressing both SCAMP2-YFP and PH-mRFP were fixed and z-series images collected (Figure 7A). Several SCAMP2-YFP dots were detected in the cells, and some of these were independent from PH-mRFP dots (Figure 7A, arrowheads). Four-dimensional (4D) analysis of SVC movement using 4D-CLSM showed that many of the SCAMP2-YFP dots were located at the side of the PH-mRFP and occasionally moved separately from the PH-mRFP positive Golgi apparatus (Figure 7B; see Supplemental Movie 1 online). To provide further evidence that SVCs exist as structures separate from TGN, BY-2 cells expressing both SCAMP2-YFP and mRFP-Rab11 were fixed and z-series images also collected (Figure 7C). Some of the SCAMP2-YFP dots were independent from mRFP-Rab11 dots (Figure 7C, arrowheads). These observations indicated that SVCs can move separately from the Golgi apparatus and TGN in the cell. Moreover, ultrastructural observation of continuous 80-nm serial sections of BY-2 cells demonstrated that SVCs were present at a distance from the Golgi stacks and the TGN (Figure 7C; see Supplemental Figures 6B and 6C online),

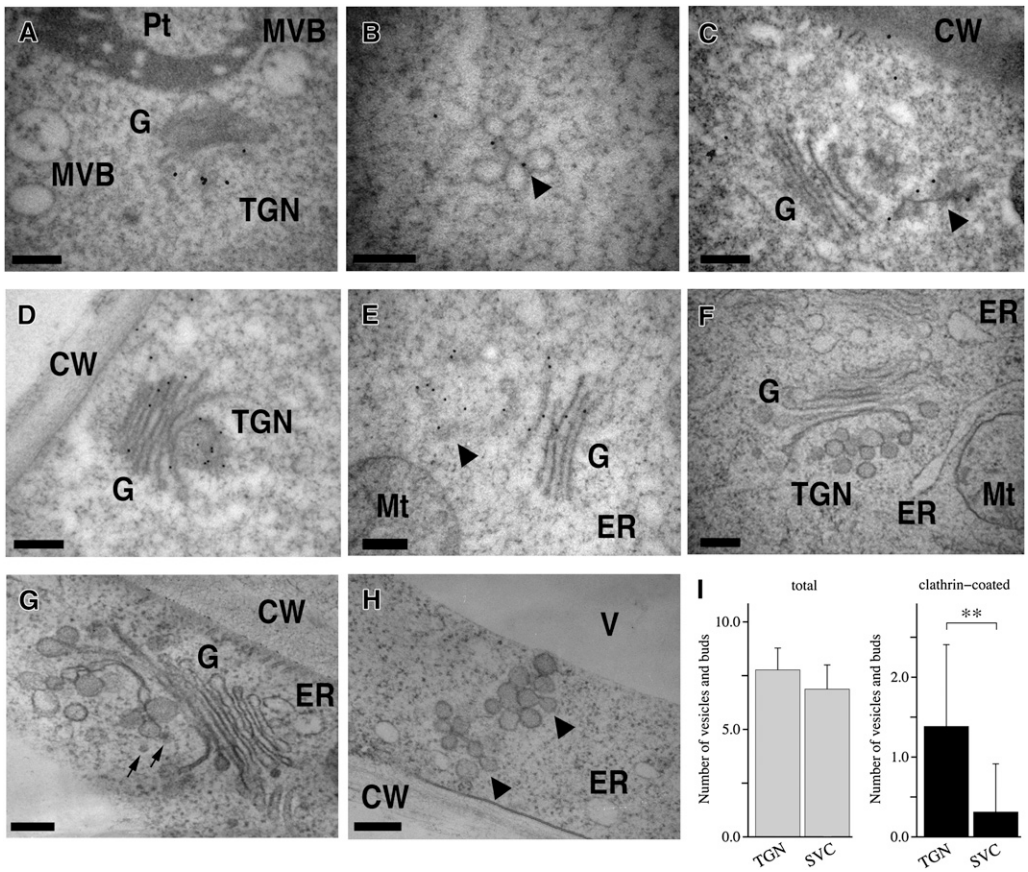

Figure 6. Immunocytochemical and Ultrastructural Analyses of Vesicle Clusters in BY-2 Cells.

(A) to **(H)** Ultrathin sections of BY-2 cells were stained using anti-SCAMP2 by immunogold labeling (**[A]** to **[C]**) or anticomplex glycan antibodies (**[D]** and **[E]**). Morphological observation of Golgi apparatus, TGN (**[F]** and **[G]**), and vesicle clusters **(H)** found in BY-2 cells. Cells were stained with tannic acid to enhance the contrast of TGN and SVC. Arrows indicate CCVs and buds. Arrowheads indicate SVC-like structures. MVB, multivesicular body; Pt, plastid; G, Golgi apparatus; Mt, mitochondrion; CW, cell wall; V, vacuole. Bars = 200 nm.

(I) Quantification of total numbers of vesicles and clathrin-coated vesicles and buds in TGN and SVC. Numbers of clathrin-coated and total vesicles and buds were counted using individual section images of TGN (n = 26) and SVC (n = 16). Error bar indicate standard error of mean. The numbers of CCVs in TGN and SVC are significantly different (Student's t test, P = 0.00011).

confirming that the SVC is a different motile compartment from the Golgi apparatus and TGN in tobacco BY-2 cells.

The positive stain with complex glycan antibody (Figure 6E) indicated that the SVC could comprise a linked cluster of secretory vesicles. To investigate the relationship between the SVC and secretion, ultrathin sections of BY-2 cells were stained with JIM7 monoclonal antibody against the homogalacturonan of pectic polysaccharides (Clausen et al., 2003). Gold signals were located on TGNs (Figure 8A, left), an SVC-like structure (Figure 8A, right; see Supplemental Figure 5F online), and on cell walls (see Supplemental Figures 5E and 5F online). The JIM7-positive vesicles were found in vesicle clusters in both TGNs and SVCs. Double immunogold labeling with anti-SCAMP2 antibody detected SCAMP2 on the membrane of JIM7 positive vesicles in both TGN and SVC (Figure 8B; see Supplemental Figure 5F online). These observations support an idea that SVCs are involved in mass secretion of cell wall materials.

To further confirm that SVC is involved in secretion, a secreted derivative of GFP that contains the signal peptide, a mutant propeptide without any targeting information, and a portion of the N-terminal region of a precursor to sweet potato (*Ipomoea batatas*) sporamin, [Spo41(I28G)-GFP] (Shimizu et al., 2005) was expressed in BY-2 cells expressing either PH-mRFP or SCAMP2-mRFP. GFP fluorescence in the culture medium was observed as previously described (Shimizu et al., 2005). The punctate distribution of the GFP signal in the cell might be the result of the presence of a propeptide region of sporamin in the construct (see Supplemental Figure 7 online and its legend). The intracellular GFP fluorescent dots colocalized almost completely with SCAMP2-mRFP (Figure 8C, middle). Many of them localized in close vicinity to PH-mRFP (Figure 8C, top), and some of them colocalized with FM4-64 signals (Figure 8C, bottom), which was observed 30 min after dye loading. These observations indicated that the SVC is indeed a compartment in the late

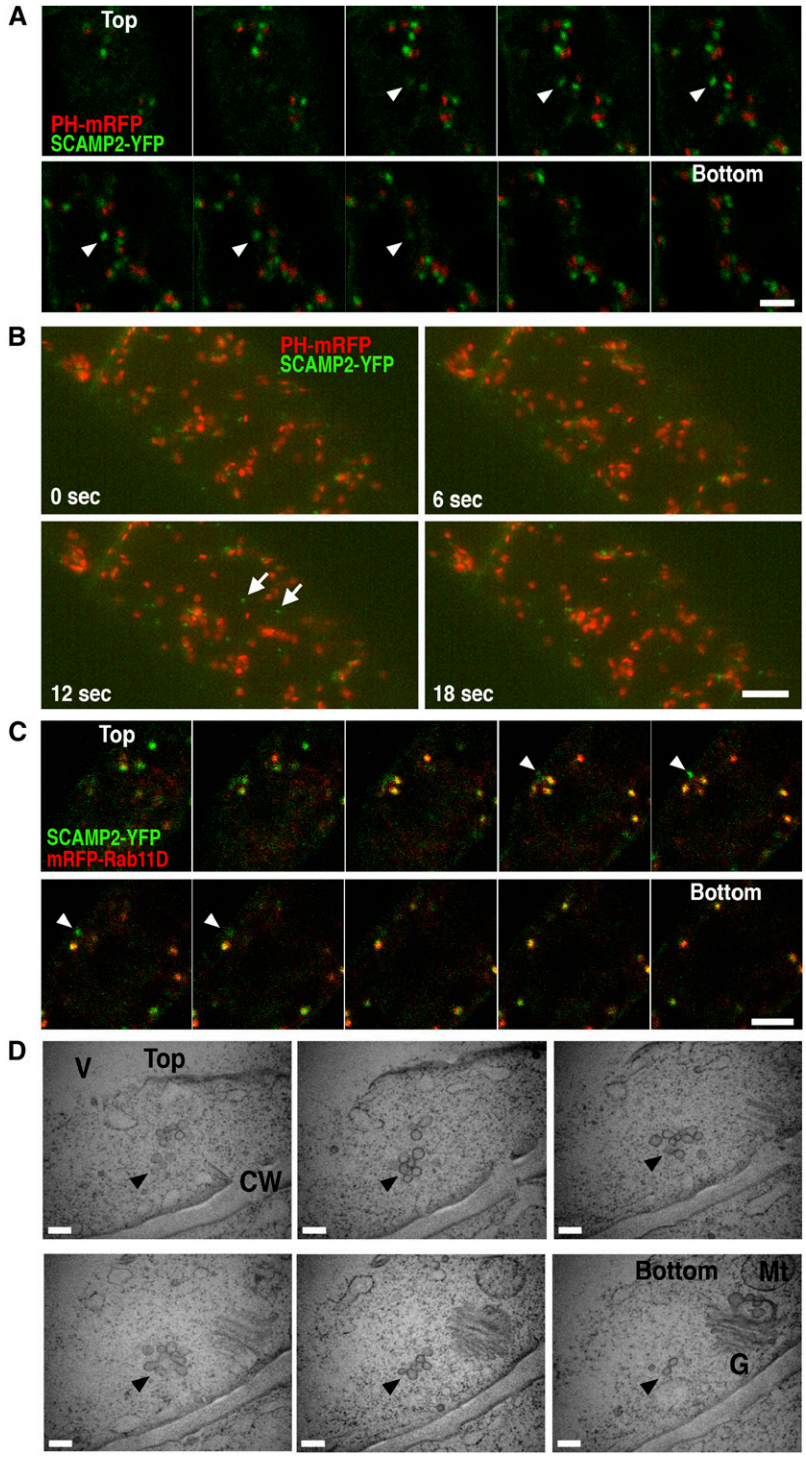

Figure 7. SVCs Are Separated from the Golgi Apparatus.

(A) A *z* axis scanning series of fixed BY-2 cells expressing PH-mRFP and SCAMP2-YFP. Arrowheads indicate SVCs.
(B) The transparency projection of three-dimensional reconstructions of a BY-2 cell expressing PH-mRFP and SCAMP2-YFP using 4D-CLSM at four time points. The panels show time-lapse pictures; arrows show SVCs. Bar = 5 μm. Movement can be seen in Supplemental Movie 1 online. Bars = 5 μm in **(A)** and **(B)**.
(C) A *z* axis scanning series of fixed BY-2 cells expressing mRFP-Rab11D and SCAMP2-YFP. Arrowheads indicate SVCs. Bar = 5 μm.
(D) Electron micrographs of 80-nm serial sections of SVCs in tobacco BY-2 cells. Arrowheads indicate SVCs. Bar = 200 nm.

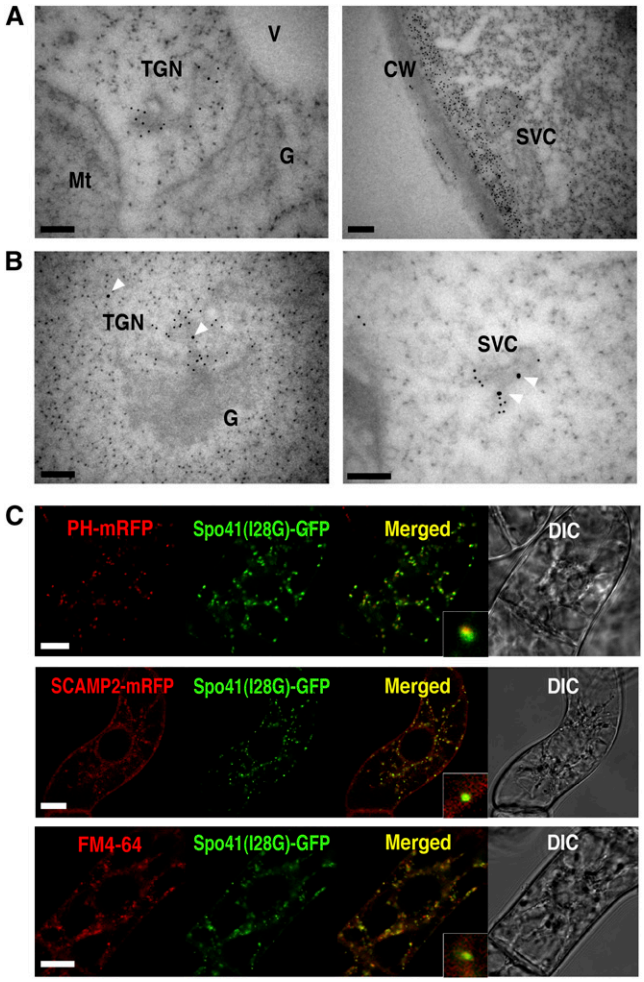

Figure 8. SVCs Contain Secretory Materials.

(A) An ultrathin section of a BY-2 cell was labeled with JIM7 antibody. Bars = 200 nm.

(B) The ultrathin section was labeled with JIM7 antibody (12 nm gold) and anti-SCAMP2 antibody (18 nm gold). Arrowheads indicate large gold particles indicating the presence of SCAMP2. CW, cell wall; V, vacuole; Mt, mitochondrion; G, Golgi. Bars = 200 nm.

(C) The secreted GFP fusion, Spo41(I28G)-GFP, was transiently expressed in BY-2 cells expressing SCAMP2-mRFP (middle) or PH-mRFP (top). Spo41(I28G)-GFP expressing BY-2 cells were incubated with FM4-64 for 30 min (bottom). Bar = 20 μm.

secretory pathway. To get another insight into the role of SVCs in secretion, we observed transformed BY-2 cells expressing both SCAMP2-YFP and PH-mRFP, using 4D-CLSM. Some SCAMP2-YFP dots quickly moved to the PM from the PH-mRFP–tagged Golgi apparatus (Figure 9A; see Supplemental Movie 2 online).

Morphological evidence of a role for SVCs in secretion was also obtained as some SVCs were observed in contact with the PM (Figure 9B) and vesicles in these SVCs were fusing with the PM (Figure 9C). In some cases, several vesicles were connected with each other to a region of the PM by electron-dense strings (Figure 9C). Taken together, these results support a conclusion that the SVC comprises a linked cluster of secretory vesicles.

To address whether the SVC is present in different cell types and plant species, the ultrastructure of tobacco root tip cells, rice cultured cells, and epidermal cells of expanding *Arabidopsis* cotyledons were also examined. All of these cell types showed the presence of SVCs (Figure 10). Additional analysis of continuous 80-nm serial sections of rice cultured cells confirmed that SVCs can exist at a distance from the Golgi stacks and TGN in these cells also (see Supplemental Figure 8 online). Moreover, SCAMP2 positive dots were observed in tobacco root cells by immunofluorescence staining using anti-SCAMP2 antibody (Figures 10E and 10F).

SVCs Are Targeted to the Cell Plate in Dividing Cells

Because secretion is important for construction of the cell plate in dividing cells, we next examined SCAMP2 localization during mitosis in BY-2 cells. During mitosis, SCAMP2 signals accumulated on newly synthesized cell plates and expanded during the progression of the cell cycle together with expansion of each cell plate (Figure 11; see Supplemental Figure 9 online). In mitotic phase cells, SCAMP2 was detected by immunostaining and as a YFP-tagged fusion and predominantly accumulated at the cell plate (Figures 10E, 10F, 11A, and 11B). Detection of tubulin with antitubulin antibody and of actin with fluorescent phalloidin in cells expressing SCAMP2-mRFP revealed that SCAMP2 localized between the opposing halves of the phragmoplast in dividing cells (see Supplemental Figures 9A and 9B online). The SCAMP2-positive cell plates at late telophase were stained by aniline blue, which confirmed that the site where SCAMP2 accumulated in mitotic cells was the cell plate containing callose (see Supplemental Figure 9C online). Interestingly, almost all of the SCAMP2-YFP signals were accumulated on cell plate in mitotic cells and were nearly devoid from the PM and the TGN (Figure 11B). This was clearly evident in sequential images taken during cell division of BY-2 cells expressing SCAMP2-mRFP (Figure 11C).

We next analyzed whether SVCs were targeted to the cell plate. When movement of SCAMP2-YFP was observed using total internal reflection fluorescence microscopy, SCAMP2-YFP–tagged dots fused rapidly and continuously with the edge or middle of the cell plate (Figure 11D; see Supplemental Movies 3 and 4 online). Tannic acid staining of ultrathin sections of dividing BY-2 cells showed that the SVCs were present in the region where the cell plate is generated (Figure 12A). This association with the cell plate was further confirmed by staining with anti-1,3-β-glucan and anti-SCAMP2 antibodies, which showed that SCAMP2-positive SVCs without 1,3-β-glucan were present on the cell plate membrane (Figure 12B). The number of SCAMP2 gold particles per 10 μm of membrane were 2.4 ± 0.74 ($n = 4$) on the PM at the side of the cells and 6.0 ± 2.0 ($n = 4$) on the cell plate, respectively. This quantification confirmed the previous fluorescence observation that SCAMP2 is largely absent from the PM in mitotic cells and suggested that most of the SCAMP2 present at the cell plates was redirected from the PM.

FM4-64 has been reported to also accumulate at the cell plate (Dettmer et al., 2006), and when FM4-64 was applied to BY-2

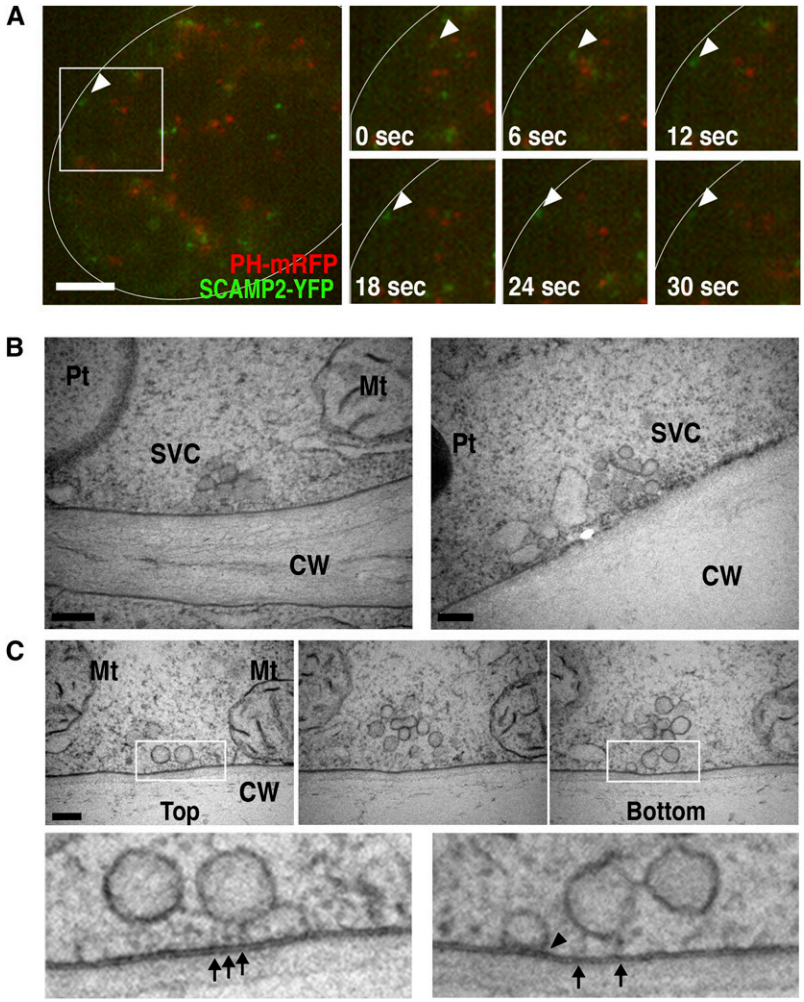

Figure 9. SVCs Are Components in the Late Secretory Pathway.

(A) Three-dimensional reconstruction of a BY-2 cell expressing PH-mRFP and SCAMP2-YFP using 4D-CLSM at six time points (right panels). The left panel shows a low magnification image at the 18 s time point with the area of the inset indicating the image shown in the right panels. White curved lines show the position of cell wall. The movement of a YFP dot to the PM is indicated by arrowheads. Movement can be seen in Supplemental Movie 2 online. Bar = 5 μm.

(B) Electron micrographs showing the fusion of an SVC with the PM.

(C) Serial sections showing the fusion of an SVC with the PM. The bottom panels show a higher magnification of the top panels. The arrowhead indicates the fusion point, and arrows show strings connected between vesicles and the PM. CW, cell wall; V, vacuole; Mt, mitochondrion; Pt, plastid. Bars = 200 nm in **(B)** and **(C)**.

cells expressing SCAMP2-YFP, the corresponding fluorescence accumulated to the cell plate in a similar manner to SCAMP2-YFP (see Supplemental Figure 10A online). This accumulation of the SCAMP2-YFP signal and the transport of SVCs to the cell plate were not inhibited by a low concentration of BFA (see Supplemental Figure 11 online), as in the case of SVCs targeted to the PM (Figure 5). Using the confocal time-lapse system, we observed that SCAMP2-YFP and FM4-64 positive SVCs were fused to the edge of the cell plate (see Supplemental Figure 10B and Supplemental Movie 5 online). These results further suggest that SCAMP2 derived from the PM is transported to the TGN by endocytosis and then targeted to the cell plate by SVCs.

DISCUSSION

The Secretory Vesicle Cluster

In this study, we analyzed the subcellular localization and transport of SCAMP2 and found a previously undescribed vesicle cluster structure, the SVC. The SVC was identified in tobacco cultured BY-2 cells as well as tobacco root tip cells, rice suspension cells, and epidermal cells of the expanding *Arabidopsis* cotyledon (Figure 10). Morphology of the SVC was clearly distinct from the MVB, as it consisted of vesicles of 50 to 100 nm in diameter in all species analyzed. Our observations that the SVC

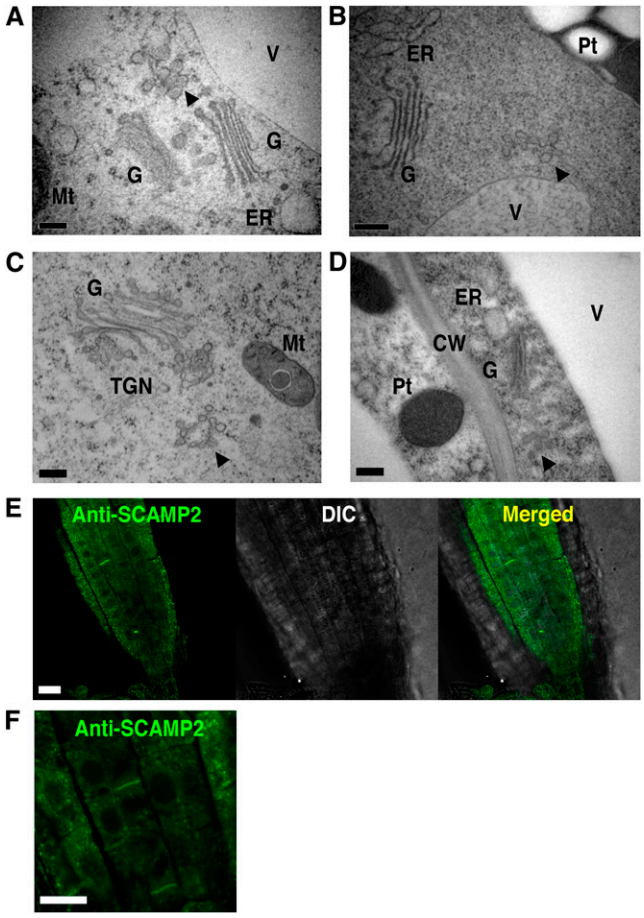

Figure 10. Morphological Observation of Several Plant Cells.

(A) to **(D)** Tobacco BY-2 cultured cells **(A)**, tobacco seedling root cell **(B)**, rice cultured cells **(C)**, and epidermal cell of growing *Arabidopsis* cotyledon **(D)**. Arrowheads show SVC. Pt, plastid; G, Golgi apparatus; Mt, mitochondrion; CW, cell wall; V, vacuole. Bars = 200 nm.

(E) Immunofluorescence staining of the mitotic zone of a tobacco root using anti-SCAMP2 antibody.

(F) Higher magnification of the root cells showing SCAMP2 localization to the developing cell plate. Bars = 10 μm in **(E)** and **(F)**.

derived from the TGN (Figures 6 and 7) contained soluble secretory proteins and cell wall components (Figure 8) generally lacked clathrin-coated structures (Figure 6I) and fused with the PM (Figures 9B and 9C) all indicated that the SVC is a motile structure at a later step of the secretory pathway. A proposed model for the generation of SVCs and SCAMP2 traffic is shown in Figure 13. First, buds and vesicles containing SCAMP2 are generated from the edges of trans-Golgi cisternae or at the TGN. During or after separation of this structure from the Golgi apparatus, the separated structure changes its shape through the budding of CCVs. The remaining structure, the SVC that we have identified, consists of a cluster of secretory vesicles. The SVC then moves to the PM in nondividing cells or to the cell plate in dividing cells. Finally, secretory vesicles in the SVC fuse with the PM or the developing cell plate. Due to the large number of vesicle fusion and tubule formation events taking place at the cell plate in dividing cells (Samuels et al., 1995), it was impossible to clearly demonstrate whether fusion of the SVC to the expanding cell plate involves a change in the clustered shape or dissociation of vesicles from the SVC prior to cell plate fusion. In any case, SCAMP2 on the PM was shown to be recycled to the trans-Golgi/TGN (Figure 5) by a route different from the MVB/PVC pathway.

In EM images, the SVC membranes show greater electron density than other membranes. This difference is especially pronounced when sections are stained with tannic acid (Figures 6F to 6H, 7C, 9B, and 9C; see Supplemental Figures 6 and 8 online). As tannic acid stains glycoproteins as well as vesicle coats, it is possible that the membrane of the SVC has a thin protein coat. We frequently observed electron-dense strings between vesicles within SVCs and between SVCs and the PM (Figure 9C). The images of SVC vesicles tethered to the PM in this manner are similar to those of coat protein I–coated vesicles tethered to the Golgi stacks (Orci et al., 1998). In the case of the Golgi apparatus, such electron-dense linear structures are known to be formed by vesicle-tethering proteins with coiled-coil structures, such as p115 and Golgins. The string between the SVC and PM might indicate the presence of such a tethering protein. In *Arabidopsis*, there are several possible coiled-coil proteins of unknown function (see http://www.coiled-coil.org/Arabidopsis/). Therefore, it will be interesting to analyze whether such coiled-coil proteins are involved in tethering of SVCs to the PM.

In this study, we used HPF/FS for EM analysis. This is a powerful method for studying membrane structure as cells are frozen in milliseconds, thus avoiding many artifacts of fixation and incubation. The ultrastructure of the TGN and partially coated reticulum in several plant species has been described using this method (Tanchak et al., 1984; Hillmer et al., 1988; Mollenhauer et al., 1991; Segui-Simarro and Staehelin, 2006). Similar analysis has been performed to monitor intracellular events during wood formation (Samuels et al., 2002). When we reexamined the images of the TGN in those reports, we observed two classes of vesicular structures at the TGN: vesicles similar to those found in SVCs and CCVs. This was also observed in tobacco cell TGNs (Figure 6G). However, such structures were scarce in SVCs located close to or fusing with the PM (Figure 6I).

CCVs in the plant TGN contain sorting receptors for vacuolar targeting (Kirsch et al., 1994). The cytosolic tails of these receptors contain motifs for interaction with adaptor proteins in CCVs (McNiven and Thompson, 2006). Thus, the TGN represents the sorting site for vacuolar delivery and secretion. Together with our observations that secretory GFP and pectin were present in the TGN and SVCs (Figure 8C), and that mature SVCs did not have vesicles with clathrin coat–like morphology, this suggests that the mature SVC formed by budding of CCVs from the TGN (Figure 13). However, we cannot rule out a possibility that some of the SVC-like images that we observed in simple sectioning were the side-cut sections of the TGN, and this possibility thus affects the quantification of the numbers of clathrin-coated buds and vesicles. Recently, Staehelin and Kang (2008) proposed two structurally different TGNs, namely, early TGN and late TGN, based on electron tomographic images of *Arabidopsis* meristem cells. The late TGNs are somehow separate structures from the Golgi apparatus but contain numbers of CCV. Therefore,

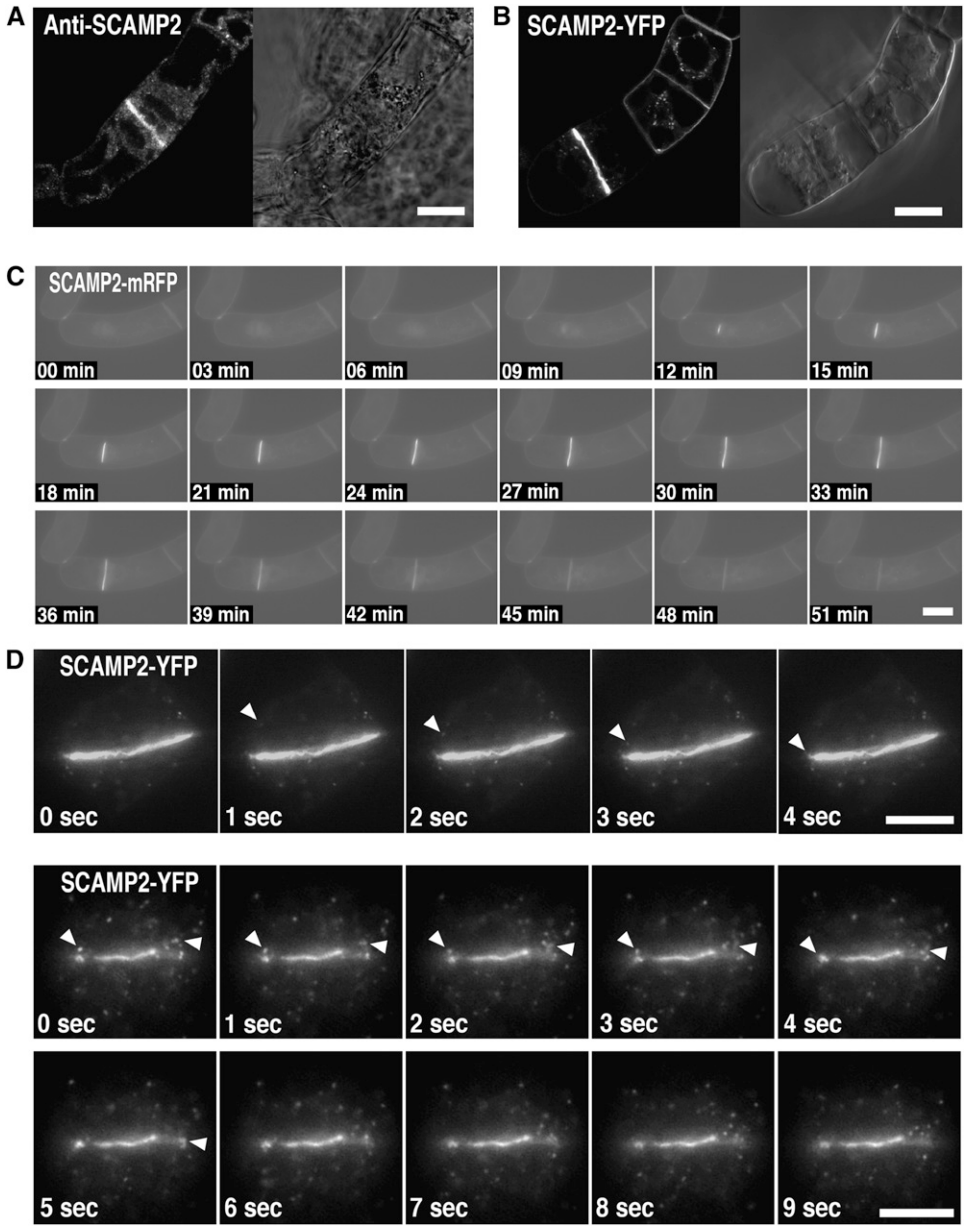

Figure 11. Movement of SVCs to the Cell Plate.

Localization of SCAMP2 in BY-2 cells at M phase.
(A) Immunofluorescence staining using anti-SCAMP2 antibody by CLSM.
(B) Fluorescence of SCAMP2-YFP was detected by CLSM.
(C) Time-lapse images of BY-2 cells expressing SCAMP2-mRFP for 50 min using video fluorescent microscopy.
(D) Time-lapse images of cell plate formation in a BY-2 cell expressing SCAMP2-YFP at 1-s intervals using total internal reflection fluorescence microscopy. Top and bottom panels show two different cell divisions. Arrowheads indicate the position of SVCs fusing with cell plates. Movement can be seen in Supplemental Movies 3 and 4 online.
Bars = 20 μm in **(A)** to **(C)** and 5 μm in **(D)**.

immature SVC may correspond to late TGN and SVC is the post-late TGN organelle generated by budding of CCV from late TGN.

During pine (*Pinus contorta*) wood formation, cell wall materials are found in TGN-like vesicle clusters (Samuels et al., 2002). As many such structures are separate from the Golgi apparatus (Figure 3E in Samuels et al., 2002), it is possible that these represent the maturing SVCs. Pine belongs to different taxonomic division from all the plants analyzed in this work; therefore, the formation of SVC in plant cells might be evolutionally conserved in a wide variety of seed-forming plants.

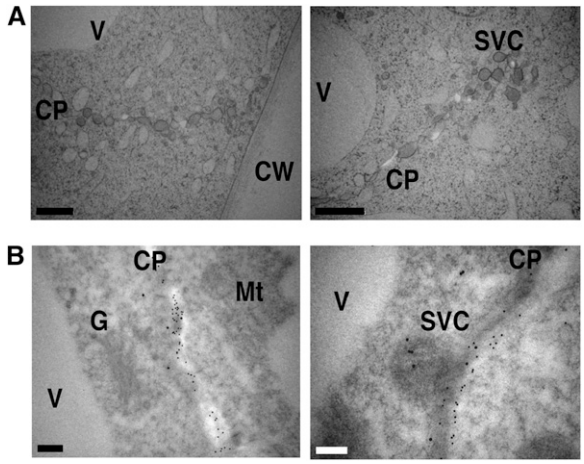

Figure 12. Immunocytochemical and Ultrastructual Analysis of Cell Plates.

(A) Electron micrographs of the cell plate region of dividing BY-2 cells.
(B) Immunogold staining of cell plate region with anti-SCAMP2 and anti-β-1,3-glucan antibodies. The 12- and 18-nm gold particles indicate the position of β-1,3-glucan and SCAMP2, respectively. CW, cell wall; G, Golgi apparatus; Mt, mitochondrion; CP, cell plate.
Bars = 500 nm **(A)** and 200 nm in **(B)**.

In *Arabidopsis* meristematic cells, the TGN is usually associated with the Golgi apparatus (Segui-Simarro and Staehelin, 2006). This difference in the location of TGN and the presence or absence of solitary TGN and SVC in *Arabidopsis* meristematic cells (Segui-Simarro and Staehelin, 2006) with the other cells used in this study and pine fiber cells can be explained by differences in cell size. Similar to many cells in crop plants, the length of cylinder-like BY-2 cells ranges from 30 to 50 μm with a diameter of 30 to 50 μm, whereas rectangular tobacco root tip cells are ~40 μm long and 30 μm wide. Rice cultured cells are spherical but somewhat irregular and have a diameter of 30 to 50 μm, *Arabidopsis* epidermal cells have an irregular shape and are ~20 μm wide and 50 μm long, whereas pine bark cells are 15 to 20 μm wide and >100 μm long. By contrast, shoot apical meristematic cells of *Arabidopsis* are roughly cubical with 4- to 5-μm sides (Segui-Simarro and Staehelin, 2006). Unlike these differences in cell sizes, the Golgi apparatus and secretory vesicles in these species are similar in size: ~500 nm wide in Golgi apparatus and 50 to 100 nm diameter in secretory vesicles, respectively. In addition, Golgi apparatus are scattered throughout the cells in all *Arabidopsis*, pine, rice, and tobacco cells. Thus, it can be calculated that it is ~10 times the distance from the Golgi apparatus to the PM in tobacco cells and other cells used in this work than in *Arabidopsis* meristematic cells. Shorter distances in *Arabidopsis* meristematic cells might limit our ability to detect any SVCs in this cell type as SVCs are transient mobile units during the final step of secretion.

Mass transport of proteins to vacuoles is mediated by large vesicles in plant cells (Hara-Nishimura et al., 1998; Toyooka et al., 2000). Although such large vesicles might be useful for the transport of large amounts of soluble and uniform contents to a final destination, such machinery is not adequate to transport large quantities of membrane proteins and lipids. By contrast, small vesicles with relatively high surface-to-volume ratios are likely to be better carriers for membrane constituents. However, transporting one vesicle with one motor protein, the mechanism found in axonal transport in neurons (Scholey, 2002), would not be an efficient system to transport massive amounts of membrane constituents. Moving arrays of tethered vesicles would be a more efficient approach to transport such vesicles efficiently. Thus, we speculate that plants developed such a transport mechanism with SVCs to deliver large quantities of lipid and membrane proteins to the PM over a long distance in relatively large plant cells.

In mammalian cells, SCAMP is involved in regulation of the insulin-responsive glucose transporter (Laurie et al., 1993) and $(Na^+, K^+)/H^+$ exchanger (Lin et al., 2005). SCAMP2 also plays an important role in the regulation of the subcellular distribution of serotonin transporters in neurons (Muller et al., 2006). Plant SVCs containing SCAMP2 might therefore also take part in the transport and regulation of transporters in plants. Recently, Jaillais et al. (2006) reported that PIN2, which is an auxin transporter, is located in a novel endomembranous compartment and auxin influx carrier AUX1 is also transported to the PM through a novel pathway distinct from PIN1 (Kleine-Vehn et al., 2006). Reichardt et al. (2007) reported that cytokinesis requires de novo secretory transport but not endocytosis using syntaxin KNOLLE as a marker. Likewise, Chow et al. (2008) reported that Rab-A2/-A3 localized to a novel post-Golgi membrane compartment contributes to the cell plate formation in *Arabidopsis* root tip cell. Thus, it will be interesting to investigate whether these proteins are localized in the SVC.

Cytokinesis and SVCs

The PM has to expand rapidly during cytokinesis in plant cells. During this period, Golgi-derived vesicles accumulate between separated chromosomes along with the cytoskeleton in a structure known as the phragmoplast. Vesicles then fuse to generate connected tubules that form into meshes and plates, collectively called the cell plate (Samuels et al., 1995; Segui-Simarro et al., 2004). Although some of the Golgi stacks move to the cell plate and its vicinity during cell division (Nebenfuhr et al., 2000), not all the Golgi do. It therefore remained unclear how Golgi-derived vesicles could be targeted efficiently to the cell plate until our discovery of SVCs in this work.

It has been reported that FM4-64 accumulates at the cell plate (Bolte et al., 2004; Dhonukshe et al., 2006). Here, we found that SCAMP2-YFP at interphase was localized in SVCs together with FM4-64 (see Supplemental Figure 8A online). Movement of the SCAMP2-YFP signal from SVCs to the cell plate was prominent at mitosis (see Supplemental Figure 10B online). As discussed above, clusters of vesicles might have an advantage for the mass transport of membranes. Thus, SVC-mediated transport to the cell plate might be an efficient transport mechanism for the generation of new PM during cytokinesis. Similar to the observed SCAMP2 localization to the cell plate, it was reported recently that ectopically expressed rice SCAMP1 is targeted to the cell plate in tobacco BY-2 cells (Lam et al., 2008). Analysis of the

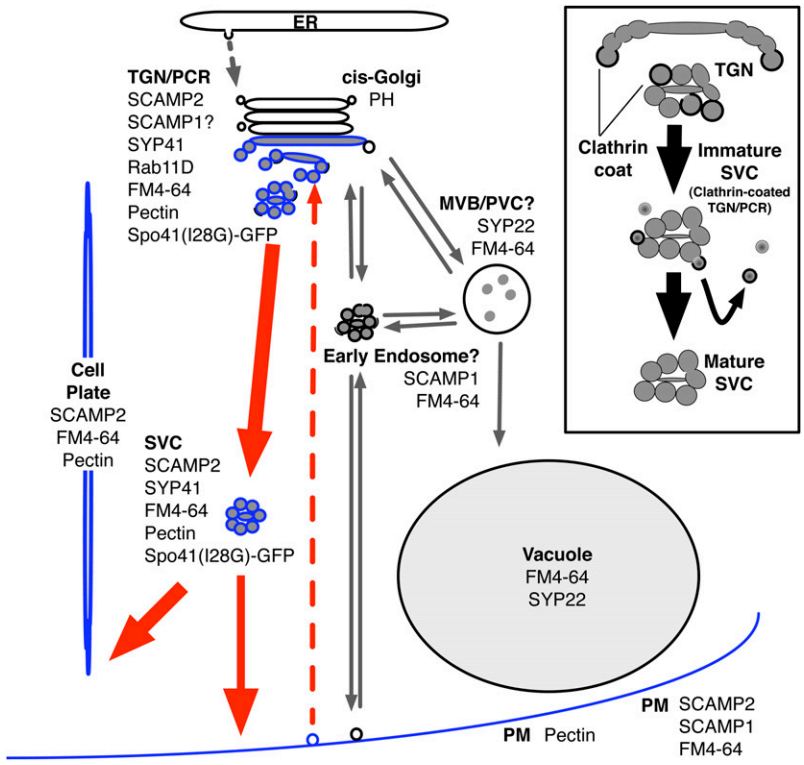

Figure 13. A Model of the Localization of SCAMP2 and the Secretory Pathway in BY-2 Cells.

SCAMP2 (blue) is localized to the trans-Golgi, TGN, PM, and SVC. The SVC separated from trans-Golgi migrates to the PM or to the cell plate membrane (see Discussion). Inset: proposed maturation pathway of the SVC.

trafficking of rice SCAMP1 in tobacco BY-2 cells indicated that this protein is transported back to clathrin-coated tubulovesicular structures from the PM, which is likely the TGN (Lam et al., 2007a). Although it is not clear how rice SCAMP1 is directed to the PM from the TGN, it is possible that some of the SVCs observed by EM could be heterogeneous and might also contain rice SCAMP1. This would be consistent with the observed varied labeling efficiency of SVCs using the anti-SCAMP2 antibody. Future characterization of endogenous SCAMP1 in tobacco BY-2 cells will clarify this possibility.

Analysis of the trafficking of membrane proteins, including the KORRIGAN protein (Zuo et al., 2000), revealed the importance of Tyr-containing motifs in cytosolic domains (Robert et al., 2005). We identified a Tyr-containing motif present in the cytosolic domain of SCAMP2 (see Supplemental Figure 1 online). This motif was conserved in plant SCAMP2 amino acid sequences and may contribute to the targeting of SCAMP2 to the cell plate.

SCAMPs and the Trafficking in Plant Cells

Subcellular fractionation analysis using a sucrose gradient indicated that SCAMP2 was broadly distributed from the PM to Golgi fractions (Figures 1 and 2D). Interestingly, both endogenous and YFP-tagged SCAMP2 showed multiple bands on SDS-polyacrylamide gels. Relative intensities of these bands differed depending on the fraction in both cases, suggesting that SCAMP2 is posttranslationally modified and that this modification may contribute the localization of this protein. It was reported previously that some mammalian SCAMPs are phosphorylated and that phosphorylation affected the localization of SCAMP3 in CHO cells (Wu and Castle, 1998). In addition, phosphorylation of the Tyr motif for endocytosis affected the localization of TrkA in mammalian cells (de Pablo et al., 2008). As plant SCAMPs have a Tyr motif in their C-terminal tail (see Supplemental Figure 1 online) and as phosphorylation of proteins tended to cause a mobility shift on SDS-polyacrylamide gels, it will be interesting to determine whether this modification is the result of the formation of multiple forms of SCAMP2 and a difference in the distribution of different forms in the cell.

The movement of FM4-64 from the PM to the TGN (Bolte et al., 2004; Figure 3; see Supplemental Figure 2 online) suggests that membrane was likely transported from the PM to TGN. It has been reported that the TGN might act as an early endosomal compartment (Dettmer et al., 2006) and that endocytosed PM and cell wall materials are used for cell plate formation via endosomes (Dettmer et al., 2006). However, our results indicated that SCAMP2 is not localized in an endosomal compartment (Figure 3A, taken at 5 to 10 min). We observed that prolonged incubation with FM4-64 allowed targeting of this dye to the TGN, where SCAMP2-YFP was also localized (Figure 3A). The discrepancy of our observation with these previous reports is probably due to a difference in temperature of incubation and

time taken to detect the internalization of FM4-64. Most studies using FM4-64 to detect endosomes used ~30 min of incubation at room temperature, a duration that allowed the dye to reach the TGN in our studies. Therefore, the TGN in tobacco BY-2 cells might not be a counterpart of the mammalian early endosome, but may function as a recycling or sorting organelle as secretory proteins pass through this compartment and SCAMP2 is localized here (Figure 4; see Supplemental Figure 3 online).

Analysis of the trafficking of rice SCAMP1 in tobacco BY-2 cells (Lam et al., 2007a) indicated that this protein localizes in a tubulovesicular endosome, which is also marked with FM4-64 and Ara7. The absence of SCAMP2 in such structures and the absence of colocalization of the early FM4-64 compartment with SCAMP2-YFP indicated that SCAMP1 and SCAMP2 are localized in distinct compartments in the early endocytic pathway. This is consistent with the observation in mammalian cells that SCAMP1 and SCAMP2 use distinct trafficking pathways, although some compartments overlap (Castle and Castle, 2005). Taken together, our data suggest the presence of at least two endocytosis routes in tobacco cells that merge in the TGN (Figure 13), one that is mediated through the FM4-64, rice SCAMP1 and Ara7-marked endosomes, and the other mediated by the SCAMP2 pathway.

METHODS

Cell Culture, Transformation, and Treatment of Cells

Culture and transformation of the tobacco (*Nicotiana tabacum*) cell line BY-2 was performed as described (Matsuoka and Nakamura, 1991). Log phase cells (3 or 4 d after culture) were used throughout the study unless otherwise stated. Stock solutions of BFA (Sigma-Aldrich), CHX (Wako Pure Chemical industries), and wortmannin (Signa-Aldrich) in DMSO were prepared at 5 mg/mL, 50 mM, and 10 mM, respectively. BFA (5 μg/mL; 17.8 μM final concentration) was added to culture medium and incubated with the cells for 2 h. In some case, after the cells had been treated with 5 μg/mL BFA for 2 h, cells were washed and transferred to fresh growth medium containing 50 μM CHX for 1 h. Control treatments were performed with equal amounts of DMSO. Alternatively, cells were incubated with 20 mM 2,3-butanedione monoxime in culture medium for 1 h. In some cases, wortmannin (16.5 μM final concentration) was added to culture medium and incubated with the cells for 1 h.

Cloning of SCAMP2 cDNA, Construction of Plasmids, and Transformation into BY-2 Tobacco Cells

A tobacco full-length enriched cDNA library was constructed from an mRNA fraction prepared from log-phase growing BY-2 cells into pGCAPsp2 vector as described (Kato et al., 2005). Full-length cDNAs for SCAMP2, SYP41, and SYP22 were isolated from the library using partial cDNA information reported previously (Matsuoka et al., 2004; Galis et al., 2006). To create the SCAMP2-mRFP, mRFP-Rab11D, and PH-mRFP fusion constructs, SCAMP2 (DDBJ accession number AB295617), Rab11D (DDBJ accession number AB470307), and PH (Yuasa et al., 2005; DDBJ accession number AB119250) cDNA were amplified by PCR from the BY-2 EST plasmids containing SCAMP2, Rab11D, or PH (Yuasa et al., 2005). See Supplemental Table 1 online for a listing of PCR primers. PCR products were then cloned into the *Bam*HI and *Kpn*I sites of pMAT330, which contains a synthetic mRFP coding sequence with plant codon usage (Toyooka et al., 2006). The fused cDNAs were placed downstream of the cauliflower mosaic virus 35S promoter in the binary vector pMAT037 and used for the *Agrobacterium tumefaciens*–mediated transformation of BY-2 cells (Matsuoka et al., 1995b). The SCAMP2-YFP, YFP-SYP41, and YFP-SYP22 were constructed using Gateway Technology (Invitrogen). Briefly, PCR products were cloned into the pENTR/D-TOPO vector using the pENTR Directional TOPO Cloning Kit (Invitrogen). The entry clone and Gateway binary vector, pH35YG2 (N-terminal YFP fusion) and pH35GY (C-terminal YFP fusion) (Kubo et al., 2005), were incubated with the LR Clonase Enzyme Mix (Invitrogen). Spo41(I28G)-GFP was prepared as described (Shimizu et al., 2005).

Antibodies

The anti-SCAMP2 antibody was raised in rabbits against the recombinant SCAMP2 protein (N-terminal 125 amino acids) prepared with the pET-Directional TOPO Expression Kit (Invitrogen) according to the manufacturer's instructions. The recombinant protein purified by Ni-Agarose was injected into a rabbit and then the serum was purified using an immobilized antigen column. The column was made using HiTrap NHS-activated Sepharose column (GE Healthcare). In some cases, IgG was purified from the serum using the Melon Gel IgG Spin Purification Kit (Pierce). The antibody against complex glycan was provided by I. Hara-Nishimura (Kyoto University, Japan). The JIM7 rat monoclonal antibody was obtained from PlantProbes. A monoclonal antibody against 1,3-β-glucan was obtained from Biosupplies Australia. The anti-PM intrinsic protein was a gift from M. Maeshima (Nagoya University, Japan) and anti-PM-ATPase was a gift from T. Sugiyama (RIKEN Plant Science Center, Japan). Anti-plant Sec61 antibody was as described (Yuasa et al., 2005). Anti-vacuolar membrane H^+-pyrophosphatase (V-PPase) antibody was raised in rabbits against the mixture of synthetic peptides (CLVGKVERNIPEDDPRNP and CGDIAGMGSDLFGSYAES, corresponding to the sequences in the fifth loop of tobacco H^+-PPase, CAA58700) conjugated with KLA, and used after affinity purification using the antigen peptides. This antibody specifically recognized an ~80-kD poloypeptide in the tonoplast. Alexa Fluor 488/568 secondary antibodies and FM 4-64 were from Invitrogen. AM 4-65 was from Biotium. The secondary antibody-conjugated alkaline phosphatase used for immunoblot analysis was obtained from Bio-Rad.

Fractionation, SDS-PAGE, and Detection of Proteins

Organelles in the microsomal fraction were separated by isopycnic ultracentrifugation, and the inosine disphosphatase activity of the fractions was measured as described (Matsuoka et al., 1995b). Proteins were separated by SDS-PAGE and analyzed by immunoblotting as described (Yuasa et al., 2005) using antibodies to plant Sec61 (1:1000), V-PPase (1:5000), anti-PM intrinsic protein (1:1000) and SCAMP2 (1:500). SCAMP2-YFP signals separated by SDS-PAGE were recorded using a Typhoon 9400 fluoroimager (GE Healthcare Bioscience) using a 488-nm excitation laser at a setting of 550 V and a 520BP40 filter.

Fluorescence Microscopy

To visualize endosomal organelles, cells were stained with 17 or 33 μM FM 4-64 or 12 μM AM4-65 dye in medium at cold or room temperature for 10 min and then washed with medium at the same temperature. Cells were then observed at 26°C. To analyze the localization of SCAMP2, BY-2 cells were washed and fixed with formaldehyde as described (Toyooka et al., 2006). Ten-day-old tobacco seedlings were fixed with formaldehyde in PBS for an hour and digested for 2 h at 30°C in 0.1% Pectolyase in water and then permeabilized for an hour in 10% DMSO and 1% Triton X-100 in PBS. Fixed cells were soaked with primary antibodies to SCAMP2 (diluted 1:100) in PBS for 1 h at room temperature, washed with PBS, and incubated with a secondary antibody diluted 1:500 in PBS.

The cells were mounted in PBS on glass slides. Living cells stably expressing YFP or mRFP fusion proteins were mounted in culture medium. These cells were observed using a CLSM system (LSM510 META, Axioplan2 Imaging; Carl Zeiss) with a Plan-Apochromat lens (63 × 1.4 oil differential interference contrast; optical slices of 1 μm). We used a 25-mW argon laser (power, 5%) with 488-nm excitation and a 505- to 530-nm band-pass filter for YFP, GFP, and Alexa Fluor 488. For FM4-64 and AM4-65, we used a 650-nm long-pass filter and 488-nm excitation. A 560-nm long-pass filter and 1- mW He-Ne laser at 80% power with 543-nm excitation was used for Alexa Fluor 568 and mRFP. Crosstalk was prevented using a multitrack configuration with line sequential scanning. Composite figures were prepared using Zeiss LSM Image Browser software. Intensity of YFP fluorescence and colocalization frequency was measured using Image J software (http://rsbweb.nih.gov/ij/).

To monitor movements of *cis*-Golgi and SVC, BY-2 cells expressing PH-mRFP and SCAMP2-YFP were observed using a 4D-CLSM (LSM5*LIVE*, Axiovert200; Carl Zeiss) with a Plan-Apochromat lens (as above). Cells were mounted in glass-bottomed dishes and scanned at a distance of 1.5 μm for 10 slices using 488- and 532-nm lasers. Time-lapse movies for cell division of BY-2 cells expressing SCAMP2-mRFP were obtained using a fluorescence microscope (Olympus; Toyooka et al., 2006). To visualize fusion of SVC with cell plate, time-lapse images of BY-2 cells expressing SCAMP2-YFP were observed using a total internal reflection fluorescence microscope (AM-TIRF; Leica) using an HCX PL APO 100 × 1.46 oil lens, YFP filter, and a DFC350FX monochrome digital camera. Cells were mounted on glass-bottomed dishes and scanned with a penetration depth of 310 nm (oblique illumination) using a 100-mW multi-argon laser. Supplemental movies were prepared using Adobe Photoshop CS2 and Apple QuickTime Pro.

HPF/FS and Tannic Acid Staining

Growing or synchronized BY-2 cells (Samuels et al., 1995) and rice (*Oryza sativa*) culture cells (Mitsui et al., 1996) were placed on a flat specimen carrier and frozen in a high-pressure freezer (EM-PACT; Leica). For morphological observations with tannic acid staining, the frozen samples were fixed with anhydrous acetone containing 2% osmic acid (OsO_4) for 3 to 4 d at −80°C. For immunocytochemistry, the frozen samples were fixed with anhydrous acetone containing 1% glutaraldehyde (GA) and 1% OsO_4 or 2% GA for 3 to 4 d at −80°C. The tubes containing the frozen samples were warmed at 3°C/h to a temperature of −20°C, at 1°C/h to a temperature of 4°C and kept for 2 h at 4°C using an automatic freeze-substitution system (EM-AFS; Leica). Fixed samples were stained with 1% tannic acid (Mallinckrodt) in acetone for 1 h at room temperature for morphological observation. The samples were washed with 100% acetone or methanol and then embedded in epoxy resin or LR White resin for morphological observations or immunological observations, respectively. For morphological observation of tobacco roots and *Arabidopsis thaliana* epidermal cells, seeds were planted in 0.8% (w/v) agar plates for 2 weeks and then moved to 2% sucrose on papers for 24 h to inhibit the formation of ice-crystal formation during HPF/FS. The roots and cotyledons were cut into 1-mm rectangles and frozen in a high-pressure freezer.

EM and Immuno-EM

Treatment of ultrathin sections fixed by GA and OsO_4 on nickel 600 mesh grids was performed as described by Follet-Gueye et al. (2003). The grids were treated with 0.5 M $NaIO_4$ for 30 min, washed twice with water (10 min each), then with 0.1 N HCl (10 min), washed with water, and then treated with 0.1 M glycine containing 0.1% Triton X-100 for 15 min. After washing with TBS, the grids were blocked with 10% BSA in TBS for 30 min at room temperature. The sections were labeled with antibodies against SCAMP2 (1:100), complex glycan (1:25), or 1,3-β-glucan (1:200) in TBS. After being washed with TBS, sections were indirectly labeled with 12- or 18-nm colloidal gold particles coupled to goat anti-rabbit IgG or anti-mouse IgG (Jackson ImmunoResearch). The ultrathin sections fixed by GA were labeled with anti-JIM7 antibody (1:100) and anti-rat IgG antibody 12 nm gold. Gold-labeled sections were washed with TBS and then rinsed in water. For morphological observations, ultrathin sections were mounted on 400 mesh Cu grids. The grids were stained with 4% aqueous uranyl acetate for 10 min and examined with a transmission electron microscope (JEOL JEM-1011) at 80 kV. Images were acquired using a Gatan DualView CCD camera and Gatan Digital Micrograph software or films. Number of gold particles on PM and cell plate were counted from sections prepared from four different blocks and measured by Image J software.

Accession Numbers

Sequence data from this article can be found in the GenBank/EMBL/DDBJ data libraries under the following accession numbers: Nt SCAMP2, DDBJ accession number AB295617; Nt SYP41, DDBJ accession number AB295618; Nt SYP22, DDBJ accession number AB295619; and Nt Rab11D, DDBJ accession number AB470307 .

Supplemental Data

The following materials are available in the online version of this article.

Supplemental Figure 1. Alignment of SCAMP2 Amino Acid Sequences.

Supplemental Figure 2. Subcellular Localization of FM4-64.

Supplemental Figure 3. Subcellular Localization of FM4-64 with Organelle Markers.

Supplemental Figure 4. Subcellular Localization of SCAMP2 in the Presence of Wortmannin.

Supplemental Figure 5. Immunogold Labeling Using Anti-SCAMP2 Antibody.

Supplemental Figure 6. Electron Micrographs of Ultrathin Serial Sections of BY-2 Cells for the Comparison of TGN and SVC.

Supplemental Figure 7. Localization of SPO41(I28G)-GFP, Sporamin Signal Peptide-GFP, and SPO41(I28G)-GFP-KDEL in Tobacco BY-2 Cells.

Supplemental Figure 8. Electron Micrographs of Ultrathin Serial Sections of Rice Culture Cells for the Comparison of TGN and SVC.

Supplemental Figure 9. Distribution of SCAMP2 and Cytoskeletones in Dividing Cells.

Supplemental Figure 10. Both SCAMP2 and FM4-64 Accumulate in the Cell Plate.

Supplemental Figure 11. Accumulation of SCAMP2-YFP and Transport of SVCs to the Cell Plate in the Presence of BFA.

Supplemental Table 1. PCR Primers.

Supplemental Movie 1. Video of Figure 7B.

Supplemental Movie 2. Video of Figure 9A.

Supplemental Movie 3. Video of Figure 11C.

Supplemental Movie 4. Video of Figure 11D.

Supplemental Movie 5. Video of Supplemental Figure 8B.

Supplemental Movie Legend.

ACKNOWLEDGMENTS

We thank Y. Suzuki, T. Narisawa, and I. Galis in RIKEN Plant Science Center for the screening of full-length cDNA clones used in this study, I.

Hara-Nishimura at Kyoto University for the complex glycan antibody, T. Demura and M. Kubo at the RIKEN Plant Science Center for the Gateway YFP fusion vectors, T. Inaba at Iwate University for the gift of GFP-PsPra3 plasmid, and S. Hamamoto at University of California, Berkeley, for the gift of tannic acid. We also thank M. Shimizu and S. Takata at the RIKEN Plant Science Center for the construction of plasmids, M. Araki and S. Oyama at the RIKEN Plant Science Center for DNA sequencing, and Derek B. Goto at Hokkaido University for improving the manuscript. This work was supported in part by grants from the Japan Society for the Promotion of Science (17770056 to K.T.) and from Grants-in-Aid for Scientific Research in Priority Areas from MEXT (17078009 to K.M.).

Received February 21, 2008; revised March 8, 2009; accepted March 30, 2009; published April 17, 2009.

REFERENCES

Bednarek, S.Y., and Falbel, T.G. (2002). Membrane trafficking during plant cytokinesis. Traffic **3:** 621–629.

Bolte, S., Talbot, C., Boutte, Y., Catrice, O., Read, N.D., and Satiat-Jeunemaitre, B. (2004). FM-dyes as experimental probes for dissecting vesicle trafficking in living plant cells. J. Microsc. **214:** 159–173.

Brand, S.H., Laurie, S.M., Mixon, M.B., and Castle, J.D. (1991). Secretory carrier membrane proteins 31–35 define a common protein composition among secretory carrier membranes. J. Biol. Chem. **266:** 18949–18957.

Castle, A., and Castle, D. (2005). Ubiquitously expressed secretory carrier membrane proteins (SCAMPs) 1-4 mark different pathways and exhibit limited constitutive trafficking to and from the cell surface. J. Cell Sci. **118:** 3769–3780.

Chow, C.M., Neto, H., Foucart, C., and Moore, I. (2008). Rab-A2 and Rab-A3 GTPases define a trans-Golgi endosomal membrane domain in *Arabidopsis* that contributes substantially to the cell plate. Plant Cell **20:** 101–123.

Clausen, M.H., Willats, W.G., and Knox, J.P. (2003). Synthetic methyl hexagalacturonate hapten inhibitors of anti-homogalacturonan monoclonal antibodies LM7, JIM5 and JIM7. Carbohydr. Res. **338:** 1797–1800.

Cosgrove, D.J. (2005). Growth of the plant cell wall. Nat. Rev. Mol. Cell Biol. **6:** 850–861.

de Pablo, Y., Perez-Garcia, M.J., Georgieva, M.V., Sanchis, D., Lindqvist, N., Soler, R.M., Comella, J.X., and Llovera, M. (2008). Tyr-701 is a new regulatory site for neurotrophin receptor TrkA trafficking and function. J. Neurochem. **104:** 124–139.

Dettmer, J., Hong-Hermesdorf, A., Stierhof, Y.D., and Schumacher, K. (2006). Vacuolar H+-ATPase activity is required for endocytic and secretory trafficking in *Arabidopsis*. Plant Cell **18:** 715–730.

Dhonukshe, P., Baluska, F., Schlicht, M., Hlavacka, A., Samaj, J., Friml, J., and Gadella, T.W., Jr. (2006). Endocytosis of cell surface material mediates cell plate formation during plant cytokinesis. Dev. Cell **10:** 137–150.

Fernandez-Chacon, R., and Sudhof, T.C. (2000). Novel SCAMPs lacking NPF repeats: ubiquitous and synaptic vesicle-specific forms implicate SCAMPs in multiple membrane-trafficking functions. J. Neurosci. **20:** 7941–7950.

Follet-Gueye, M.L., Pagny, S., Faye, L., Gomord, V., and Driouich, A. (2003). An improved chemical fixation method suitable for immunogold localization of green fluorescent protein in the Golgi apparatus of tobacco Bright Yellow (BY-2) cells. J. Histochem. Cytochem. **51:** 931–940.

Foresti, O., daSilva, L.L., and Denecke, J. (2006). Overexpression of the Arabidopsis syntaxin PEP12/SYP21 inhibits transport from the prevacuolar compartment to the lytic vacuole in vivo. Plant Cell **18:** 2275–2293.

Galis, I., Simek, P., Narisawa, T., Sasaki, M., Horiguchi, T., Fukuda, H., and Matsuoka, K. (2006). A novel R2R3 MYB transcription factor NtMYBJS1 is a methyl jasmonate-dependent regulator of phenylpropanoid-conjugate biosynthesis in tobacco. Plant J. **46:** 573–592.

Hara-Nishimura, I.I., Shimada, T., Hatano, K., Takeuchi, Y., and Nishimura, M. (1998). Transport of storage proteins to protein storage vacuoles is mediated by large precursor-accumulating vesicles. Plant Cell **10:** 825–836.

Higaki, T., Kutsuna, N., Okubo, E., Sano, T., and Hasezawa, S. (2006). Actin microfilaments regulate vacuolar structures and dynamics: Dual observation of actin microfilaments and vacuolar membrane in living tobacco BY-2 Cells. Plant Cell Physiol. **47:** 839–852.

Hillmer, S., Freundt, H., and Robinson, D.G. (1988). The partially coated riticulum and its relationship to the Golgi apparatus in higher plant cells. Eur. J. Cell Biol. **47:** 206–212.

Inaba, T., Nagano, Y., Nagasaki, T., and Sasaki, Y. (2002). Distinct localization of two closely related Ypt3/Rab11 proteins on the trafficking pathway in higher plants. J. Biol. Chem. **277:** 9183–9188.

Jaillais, Y., Fobis-Loisy, I., Miege, C., Rollin, C., and Gaude, T. (2006). AtSNX1 defines an endosome for auxin-carrier trafficking in Arabidopsis. Nature **443:** 106–109.

Kato, S., Ohtoko, K., Ohtake, H., and Kimura, T. (2005). Vector-capping: A simple method for preparing a high-quality full-length cDNA library. DNA Res. **12:** 53–62.

Kirsch, T., Paris, N., Butler, J.M., Beevers, L., and Rogers, J.C. (1994). Purification and initial characterization of a potential plant vacuolar targeting receptor. Proc. Natl. Acad. Sci. USA **91:** 3403–3407.

Kleine-Vehn, J., Dhonukshe, P., Swarup, R., Bennett, M., and Friml, J. (2006). Subcellular trafficking of the *Arabidopsis* auxin influx carrier AUX1 uses a novel pathway distinct from PIN1. Plant Cell **18:** 3171–3181.

Kubo, M., Udagawa, M., Nishikubo, N., Horiguchi, G., Yamaguchi, M., Ito, J., Mimura, T., Fukuda, H., and Demura, T. (2005). Transcription switches for protoxylem and metaxylem vessel formation. Genes Dev. **19:** 1855–1860.

Lam, S.K., Cai, Y., Hillmer, S., Robinson, D.G., and Jiang, L. (2008). SCAMPs highlight the developing cell plate during cytokinesis in tobacco BY-2 cells. Plant Physiol. **147:** 1637–1645.

Lam, S.K., Siu, C.L., Hillmer, S., Jang, S., An, G., Robinson, D.G., and Jiang, L. (2007a). Rice SCAMP1 defines clathrin-coated, trans-Golgi-located tubular-vesicular structures as an early endosome in tobacco BY-2 cells. Plant Cell **19:** 296–319.

Lam, S.K., Tse, Y.C., Robinson, D.G., and Jiang, L. (2007b). Tracking down the elusive early endosome. Trends Plant Sci. **12:** 497–505.

Laurie, S.M., Cain, C.C., Lienhard, G.E., and Castle, J.D. (1993). The glucose transporter GluT4 and secretory carrier membrane proteins (SCAMPs) colocalize in rat adipocytes and partially segregate during insulin stimulation. J. Biol. Chem. **268:** 19110–19117.

Lin, P.J., Williams, W.P., Luu, Y., Molday, R.S., Orlowski, J., and Numata, M. (2005). Secretory carrier membrane proteins interact and regulate trafficking of the organellar (Na+,K+)/H+ exchanger NHE7. J. Cell Sci. **118:** 1885–1897.

Liu, L., Guo, Z., Tieu, Q., Castle, A., and Castle, D. (2002). Role of secretory carrier membrane protein SCAMP2 in granule exocytosis. Mol. Biol. Cell **13:** 4266–4278.

Matsuoka, K., Bassham, D.C., Raikhel, N.V., and Nakamura, K.

(1995a). Different sensitivity to wortmannin of two vacuolar sorting signals indicates the presence of distinct sorting machineries in tobacco cells. J. Cell Biol. **130:** 1307–1318.

Matsuoka, K., Demura, T., Galis, I., Horiguchi, T., Sasaki, M., Tashiro, G., and Fukuda, H. (2004). A comprehensive gene expression analysis toward the understanding of growth and differentiation of tobacco BY-2 cells. Plant Cell Physiol. **45:** 1280–1289.

Matsuoka, K., Higuchi, T., Maeshima, M., and Nakamura, K. (1997). A vacuolar-type H+-ATPase in a nonvacuolar organelle is required for the sorting of soluble vacuolar protein precursors in tobacco cells. Plant Cell **9:** 533–546.

Matsuoka, K., and Nakamura, K. (1991). Propeptide of a precursor to a plant vacuolar protein required for vacuolar targeting. Proc. Natl. Acad. Sci. USA **88:** 834–838.

Matsuoka, K., Watanabe, N., and Nakamura, K. (1995b). O-glycosylation of a precursor to a sweet potato vacuolar protein, sporamin, expressed in tobacco cells. Plant J. **8:** 877–889.

McNiven, M.A., and Thompson, H.M. (2006). Vesicle formation at the plasma membrane and trans-Golgi network: The same but different. Science **313:** 1591–1594.

Mitsui, T., Yamaguchi, J., and Akazawa, T. (1996). Physicochemical and serological characterization of rice alpha-amylase isoforms and identification of their corresponding genes. Plant Physiol. **110:** 1395–1404.

Mollenhauer, H.H., Morre, D.J., and Griffing, L.R. (1991). Post Golgi apparatus structures and membrane removal in plants. Protoplasma **162:** 55–60.

Muller, H.K., Wiborg, O., and Haase, J. (2006). Subcellular redistribution of the serotonin transporter by secretory carrier membrane protein 2. J. Biol. Chem. **281:** 28901–28909.

Nebenfuhr, A., Frohlick, J.A., and Staehelin, L.A. (2000). Redistribution of Golgi stacks and other organelles during mitosis and cytokinesis in plant cells. Plant Physiol. **124:** 135–151.

Nebenfuhr, A., Gallagher, L.A., Dunahay, T.G., Frohlick, J.A., Mazurkiewicz, A.M., Meehl, J.B., and Staehelin, L.A. (1999). Stop-and-go movements of plant Golgi stacks are mediated by the acto-myosin system. Plant Physiol. **121:** 1127–1142.

Orci, L., Perrelet, A., and Rothman, J.E. (1998). Vesicles on strings: Morphological evidence for processive transport within the Golgi stack. Proc. Natl. Acad. Sci. USA **95:** 2279–2283.

Reichardt, I., Stierhof, Y.D., Mayer, U., Richter, S., Schwarz, H., Schumacher, K., and Jurgens, G. (2007). Plant cytokinesis requires de novo secretory trafficking but not endocytosis. Curr. Biol. **17:** 2047–2053.

Robert, S., Bichet, A., Grandjean, O., Kierzkowski, D., Satiat-Jeunemaitre, B., Pelletier, S., Hauser, M.T., Hofte, H., and Vernhettes, S. (2005). An *Arabidopsis* endo-1,4-beta-D-glucanase involved in cellulose synthesis undergoes regulated intracellular cycling. Plant Cell **17:** 3378–3389.

Rojo, E., and Denecke, J. (2008). What is moving in the secretory pathway of plants? Plant Physiol. **147:** 1493–1503.

Saint-Jore-Dupas, C., Gomord, V., and Paris, N. (2004). Protein localization in the plant Golgi apparatus and the trans-Golgi network. Cell. Mol. Life Sci. **61:** 159–171.

Samaj, J., Baluska, F., Voigt, B., Schlicht, M., Volkmann, D., and Menzel, D. (2004). Endocytosis, actin cytoskeleton, and signaling. Plant Physiol. **135:** 1150–1161.

Samuels, A.L., Giddings, T.H., Jr., and Staehelin, L.A. (1995). Cytokinesis in tobacco BY-2 and root tip cells: A new model of cell plate formation in higher plants. J. Cell Biol. **130:** 1345–1357.

Samuels, A.L., Rensing, K.H., Douglas, C.J., Mansfield, S.D., Dharmawardhana, D.P., and Ellis, B.E. (2002). Cellular machinery of wood production: differentiation of secondary xylem in *Pinus contorta* var. latifolia. Planta **216:** 72–82.

Scholey, J.M. (2002). Rafting along the axon on Unc104 motors. Dev. Cell **2:** 515–516.

Segui-Simarro, J.M., Austin II, J.R., White, E.A., and Staehelin, L.A. (2004). Electron tomographic analysis of somatic cell plate formation in meristematic cells of *Arabidopsis* preserved by high-pressure freezing. Plant Cell **16:** 836–856.

Segui-Simarro, J.M., and Staehelin, L.A. (2006). Cell cycle-dependent changes in Golgi stacks, vacuoles, clathrin-coated vesicles and multivesicular bodies in meristematic cells of *Arabidopsis thaliana*: A quantitative and spatial analysis. Planta **223:** 223–236.

Shimizu, M., Igasaki, T., Yamada, M., Yuasa, K., Hasegawa, J., Kato, T., Tsukagoshi, H., Nakamura, K., Fukuda, H., and Matsuoka, K. (2005). Experimental determination of proline hydroxylation and hydroxyproline arabinogalactosylation motifs in secretory proteins. Plant J. **42:** 877–889.

Staehelin, L.A., and Kang, B.H. (2008). Nanoscale architecture of endoplasmic reticulum export sites and of Golgi membranes as determined by electron tomography. Plant Physiol. **147:** 1454–1468.

Surpin, M., and Raikhel, N. (2004). Traffic jams affect plant development and signal transduction. Nat. Rev. Mol. Cell Biol. **5:** 100–109.

Takamori, S., et al. (2006). Molecular anatomy of a trafficking organelle. Cell **127:** 831–846.

Tanchak, M.A., Griffing, L.R., Mersey, B.G., and Fowke, L.C. (1984). Endocytosis of cationized ferritin by coated vesicles of soybean protoplasts. Planta **162:** 481–486.

Toyooka, K., Moriyasu, Y., Goto, Y., Takeuchi, M., Fukuda, H., and Matsuoka, K. (2006). Protein aggregates are transported to vacuoles by a macroautophagic mechanism in nutrient-starved plant cells. Autophagy **2:** 96–106.

Toyooka, K., Okamoto, T., and Minamikawa, T. (2000). Mass transport of proform of a KDEL-tailed cysteine proteinase (SH-EP) to protein storage vacuoles by endoplasmic reticulum-derived vesicle is involved in protein mobilization in germinating seeds. J. Cell Biol. **148:** 453–464.

Uemura, T., Ueda, T., Ohniwa, R.L., Nakano, A., Takeyasu, K., and Sato, M.H. (2004). Systematic analysis of SNARE molecules in Arabidopsis: Dissection of the post-Golgi network in plant cells. Cell Struct. Funct. **29:** 49–65.

Wu, T.T., and Castle, J.D. (1998). Tyrosine phosphorylation of selected secretory carrier membrane proteins, SCAMP1 and SCAMP3, and association with the EGF receptor. Mol. Biol. Cell **9:** 1661–1674.

Yuasa, K., Toyooka, K., Fukuda, H., and Matsuoka, K. (2005). Membrane-anchored prolyl hydroxylase with an export signal from the endoplasmic reticulum. Plant J. **41:** 81–94.

Zuo, J., Niu, Q.W., Nishizawa, N., Wu, Y., Kost, B., and Chua, N.H. (2000). KORRIGAN, an Arabidopsis endo-1,4-beta-glucanase, localizes to the cell plate by polarized targeting and is essential for cytokinesis. Plant Cell **12:** 1137–1152.